PHYSICAL REVIEW D **72,** 125005 (2005)

Asymptotic thermal quark masses and the entropy of QCD in the large-N_f limit

Jean-Paul Blaizot and Andreas Ipp
ECT, Villa Tambosi, Strada delle Tabarelle 286, I-38050 Villazzano Trento, Italy*

Anton Rebhan and Urko Reinosa
Institut für Theoretische Physik, Technische Universität Wien, Wiedner Hauptstraße 8-10, A-1040 Vienna, Austria
(Received 4 November 2005; published 15 December 2005)

We study the thermodynamics of QCD in the limit of large flavor number (N_f) and test the proposal to resum the physics of hard thermal loops (HTL) through a nonperturbative expression for the entropy obtained from a Φ-derivable two-loop approximation. The fermionic contribution to the entropy involves a full next-to-leading order evaluation of the asymptotic thermal quark mass, which is nonlocal, and for which only a weighted average value was known previously. For a natural choice of renormalization scale we find remarkably good agreement of the next-to-leading order HTL results for the fermion self-energy and in turn for the entropy with the respective exact large-N_f results, even at very large coupling.

DOI: 10.1103/PhysRevD.72.125005 PACS numbers: 11.10.Wx, 11.15.Pg, 12.38.Mh

I. INTRODUCTION

The perturbative series for the thermodynamic potentials of hot QCD is by now known up to and including order $g^6\log(g)$ [1–4], with $g=\sqrt{4\pi\alpha_s}$ being the Yang-Mills coupling constant. Taken at face value, this series is poorly convergent and suffers from a strong dependence on the renormalization point even at temperatures many orders of magnitude higher than the QCD scale $\Lambda_{\rm QCD}$. However, this problem is not specific to QCD at high temperature, which has a nonperturbative sector starting to contribute at order g^6. Similarly poor convergence behavior appears also in simple scalar field theory [5], and even in the case of large-N ϕ^4 theory [6], where all interactions can be resummed in a local thermal mass term, as soon as one starts expanding out in a series of powers and logarithms of the coupling.

Various mathematical extrapolation techniques have been tried to restore the convergence of the perturbative series, such as Padé approximants [7–9], self-similar approximants [10], and Borel resummation [11,12]. A more physically motivated proposal for reorganizing thermal perturbation theories is called ''screened perturbation theory'' [13,14]. This is a variant of a variational perturbation theory, where the tree-level Lagrangian is modified so that it includes a mass term, which is then determined by a variational principle (minimal sensitivity). In the case of gauge theories, the prefactor of the gauge-invariant nonlocal and nonlinear hard-thermal-loop (HTL) action [15,16] is used for this purpose in a generalization of this approach to QCD by Andersen, Braaten, Petitgirard, and Strickland [17–20].

The HTL action is the correct leading-order effective action for soft modes at energies parametrically smaller than the temperature. However it is somewhat problematic to also use it at hard scales, which are responsible for the leading terms in the thermodynamic potential, albeit the problems with thermal perturbation theory clearly come from screening effects at soft scales. Indeed (HTL)screened perturbation theory changes the ultraviolet structure and requires an *ad hoc* renormalization of additional UV singularities.

An alternative proposal for resumming the physics of hard thermal loops was put forward in Refs. [21–24][1] and is based on a nonperturbative expression for the entropy density that can be obtained from a Φ-derivable two-loop approximation [26]. Here the emphasis is fully on a quasiparticle picture, whose residual interactions are assumed to be weak after the bulk of the interaction effects have been incorporated in the spectral data of the quasiparticles. As opposed to methods based on ''screened perturbation theory,'' Φ-derivable approximations have better properties with respect to renormalization. They are renormalizable in the case of scalar field theories [27–32], although in gauge theories the question of renormalizability remains still open. However, when combined with HTL approximations, they define UV finite physical quantities without introducing spurious counterterms [21–23].

These approaches indeed succeed in taming the plasmon term $\sim g^3$ that spoils the apparent convergence of strict perturbative expansions in g and comparison with existing lattice data suggest that the entropy of QCD for $T\geq 3T_c$ can indeed be accounted for remarkably well when the leading-order interactions are resummed into spectral properties of HTL quasiparticles [21–23].

Since this success is gauged mostly from the comparison with lattice data, it is desirable to have other possibilities for testing these resummation prescriptions. In Ref. [33] it was suggested to use the large flavor-number (N_f) limit of QED and QCD for that purpose. The thermodynamic potential has been worked out in Ref. [33–35] to order

[1]For an attempt to achieve a comparable resummation directly in terms of the pressure see [25].

N_f^0 and to all orders in g^2N_f, which is kept finite as the limit $N_f \to \infty$, $g \to 0$ is taken.

Large-N_f QCD is no longer asymptotically free. In this limit the renormalization scale dependence is determined (nonperturbatively) by the one-loop beta function according to

$$\frac{1}{g^2_{\rm eff}(\mu)} = \frac{1}{g^2_{\rm eff}(\mu')} + \frac{\log(\mu'/\mu)}{6\pi^2}, \tag{1}$$

where we have defined $g^2_{\rm eff} = g^2N_f/2$ (in QED we would have $g^2_{\rm eff} = g^2N_f$). There is a Landau singularity in the vacuum gauge field propagator at $Q^2 = \Lambda_{\rm L}^2$ with

$$\Lambda_{\rm L} = \bar{\mu}_{\rm MS} e^{5/6} e^{6\pi^2/g^2_{\rm eff}(\bar{\mu}_{\rm MS})}, \tag{2}$$

where $\bar{\mu}_{\overline{\rm MS}}$ is the scale of modified minimal subtraction. However, although the large-N_f theory has an unavoidable ambiguity associated with its UV completion, in the thermodynamic potential the magnitude of the ambiguity is suppressed by a factor $(T/\Lambda_{\rm L})^4$, which in practice means that the Landau pole problem can be ignored for all couplings $g_{\rm eff}(\bar{\mu}_{\overline{\rm MS}} = \pi T) \lesssim 6$. Since strict perturbation theory appears to work only for $g_{\rm eff} \lesssim 2$, this gives enough room for testing improvements of thermal perturbation theory.

In this paper we shall test the HTL resummation proposed in Refs. [21–23], which use the nonperturbative expression for the entropy obtained from a Φ-derivable two-loop approximation. In the large-N_f limit, a complete HTL resummation involves, in particular, the evaluation of next-to-leading order (NLO) thermal quark masses at asymptotic hard scales. In one-loop HTL-resummed perturbation theory, these thermal masses are nonlocal, i.e. functions of momentum, and so far only a certain weighted average was known, and this only to next-to-leading order in the coupling. In this paper we shall perform a complete HTL evaluation, which resums an infinite series in the coupling, and we compare with the numerical evaluation of the exact large-N_f values. A corresponding evaluation of the entropy shows considerable improvement compared to a previous evaluation using the averaged asymptotic masses at next-to-leading order in HTL-resummed perturbation theory [36]. Although at larger coupling the HTL results have a large renormalization scale dependence, choosing the scale of fastest apparent convergence reproduces the exact large-N_f result for all $g^2_{\rm eff}$ with a quality comparable to an optimized g^6 result [35].

The organization of this paper is as follows: In Sec. II we first review the Φ-derivable approximation to the entropy. At two-loop order we present the remarkably simple quasiparticle formulas for the entropy and number density which can be used both in the large-N_f limit and for an HTL approximation. In Sec. III we discuss the issue of renormalization both from the perspective of the thermodynamic potential and of the quasiparticle entropy and number density. In Sec. IV we evaluate the fermion self-energy, which plays a central role in the quasiparticle entropy expressions, and which requires to solve a technical problem related to the necessity of eliminating the Landau pole by a momentum cutoff. Such a cutoff has to be imposed in a way which respects Euclidean rotational invariance in order to avoid spurious contributions in already renormalized expressions [derived in dimensional regularization as we shall use modified minimal subtraction ($\overline{\rm MS}$)]. Since the quasiparticle entropy is formulated in Minkowski space, this requirement leads to intricacies in the numerical evaluation, whose results are finally given in Sec. V. There we present the numerical results for the complete large-N_f entropy and the complete momentum-dependent asymptotic thermal quark masses together with their respective HTL approximations. We find remarkable agreement of the latter with the exact results provided the HTL approximation is used in a nonperturbative manner (i.e., not truncating at the order of perturbative accuracy) and an optimized renormalization scale is chosen. In this case, the agreement is comparable to optimized results using perturbative results through order g^6.

At this point it is useful to specify the notation to be used throughout the paper. As gauge group we take SU(N), so N denotes the number of quark colors. As already said, N_f is the number of quark flavors. The number of gluons is denoted by $N_g = N^2 - 1$. We use the Minkowski metric $g^{\mu\nu} = (+, -, -, -)$ and denote by capital letters 4-momenta P with components $P^\mu = (p_0, \mathbf{p})$, so that $P^2 = p_0^2 - \mathbf{p}^2$. In finite temperature calculations, we are led to set $p_0 = i\omega_n$, where ω_n is a Matsubara frequency ($\omega_n = n\pi\beta$ where n is an even integer for bosons and odd integer for fermions). We shall denote the typical sum integrals that occur at finite temperature by the following shorthand notation:

$$\sum\!\!\!\!\!\!\int_P f(P) = \frac{1}{\beta}\sum_n \int \frac{d^3p}{(2\pi)^3} f(i\omega_n, \mathbf{p}). \tag{3}$$

At zero temperature, the sum over Matsubara frequencies is replaced by an integral over the imaginary energy axis, leading to an Euclidean integral denoted by

$$\int_{P_{\rm E}} f(P) = \int_{-i\infty}^{i\infty} \frac{dp_0}{2\pi i} \int \frac{d^3p}{(2\pi)^3} f(p_0, \mathbf{p}). \tag{4}$$

For an integral over the four components of a four-vector, we simply write

$$\int_P f(P) = \int_{-\infty}^{\infty} \frac{dp_0}{2\pi} \int \frac{d^3p}{(2\pi)^3} f(p_0, \mathbf{p}) = \int_{p_0}\int_{\mathbf{p}} f(P). \tag{5}$$

We denote the free propagator by $\Delta_0(P) = -1/(P^2 - M^2)$ or, in its spectral representation, by

$$\Delta_0(\omega, p) = \int_{p_0} \frac{\rho_0(P)}{p_0 - \omega}, \tag{6}$$

where ω is a complex energy variable, and the spectral function is $\rho_0(P) = 2\pi\epsilon(p_0)\delta(P^2 - M^2)$. The free fermion propagator is then given by $S_0(P) = (\not{p} + M)\Delta_0(P)$ or, in its spectral form, by

$$S_0(\omega, p) = \int_{p_0} \frac{(\not{p} + M)\rho_0(P)}{p_0 - \omega}, \tag{7}$$

where we used the fact that $\rho_0(P)$ is an odd function in p_0 to replace $\omega\gamma_0$ by $p_0\gamma_0$ in $\not{p}$ within the integral.

II. Φ-DERIVABLE TWO-LOOP ENTROPY AND HTL RESUMMATION

A. Generalities

Φ-derivable approximations [37] are constructed from the two-particle-irreducible (2PI) skeleton expansion [38,39]. In the latter, the thermodynamic potential is expressed in terms of dressed propagators (G for bosons, S for fermions) according to

$$\Omega[G, S] = \tfrac{1}{2}T\,\mathrm{Tr}\log G^{-1} - \tfrac{1}{2}T\,\mathrm{Tr}\,\Pi G - T\,\mathrm{Tr}\log S^{-1} + T\,\mathrm{Tr}\,\Sigma S + T\Phi[G, S], \tag{8}$$

where "Tr" refers to full functional traces $\mathrm{Tr} = \mathrm{tr}\int_0^\beta d\tau \times \int_{\mathbf{x}} \to \beta V\,\mathrm{tr}\sum_K$ and $\Phi[G, S]$ is the sum of 2-particle-irreducible "skeleton" diagrams. In gauge theories, one either has to assume a ghost-free gauge such as temporal axial gauge or to include the bosonic Faddeev-Popov ghost propagator G_{gh}. For simplicity we shall assume a ghost-free gauge in the general discussion. At both the level of HTL approximations and in the large-N_f limit, we can and shall use the Coulomb gauge for this purpose instead of the somewhat problematic [40] temporal axial gauge.

Standard contour integration gives

$$\Omega[G, S]/V = \mathrm{tr}\int_K n(k_0)\,\mathrm{Im}[\log G^{-1}(K) - \Pi(K)G(K)] + 2\,\mathrm{tr}\int_K f(k_0)\,\mathrm{Im}[\log S^{-1}(K) - \Sigma(K)S(K)] + T\Phi[G, S]/V, \tag{9}$$

where tr denotes a trace over discrete labels only. The Bose-Einstein and Fermi-Dirac factors are defined as $n(\omega) = (e^{\omega/T} - 1)^{-1}$ and $f(\omega) = (e^{(\omega-\mu)/T} + 1)^{-1}$, respectively.

The self-energies $\Pi = G^{-1} - G_0^{-1}$ and $\Sigma = S^{-1} - S_0^{-1}$, where G_0 and S_0 are bare propagators, are themselves functionals of the full propagators. They are determined by the stationarity property,

$$\delta\Omega[G, S]/\delta G = 0 = \delta\Omega[G, S]/\delta S, \tag{10}$$

according to

$$\delta\Phi[G, S]/\delta G = \tfrac{1}{2}\Pi, \qquad \delta\Phi[G, S]/\delta S = -\Sigma. \tag{11}$$

The Φ-derivable two-loop approximation consists of keeping only the two-loop skeleton diagrams (see Fig. 1), which leads to a dressed one-loop approximation for the self-energies (11). In a gauge theory this generally introduces gauge dependences (which are parametrically suppressed, though [41]). However, the further approximations put forward in Refs. [21–23] are manifestly gauge independent in the Φ-derivable two-loop approximation.

A self-consistent two-loop approximation for Ω has a remarkable consequence for the first derivatives of the thermodynamic potential, the entropy and the number densities:

$$S = \frac{\partial P}{\partial T}\bigg|_\mu, \qquad \mathcal{N} = \frac{\partial P}{\partial \mu}\bigg|_T, \qquad P = -\Omega/V. \tag{12}$$

Because of the stationarity property (10), one can ignore the T and μ dependences implicit in the spectral densities of the full propagators, and differentiate exclusively the statistical distribution functions n and f in (9). Now the derivative of the *two-loop* functional $T\Phi[G, S]$ at fixed spectral densities of the propagators G and S turns out to cancel part of the terms $\mathrm{Im}(\Pi G)$ and $\mathrm{Im}(\Sigma S)$ in (9):

$$S'_{2\text{-loop}} \equiv -\frac{\partial(T\Phi_{2\text{-loop}})}{\partial T}\bigg|_{G,S} + \mathrm{tr}\int_K \bigg[\frac{\partial n(k_0)}{\partial T}\,\mathrm{Re}\,\Pi\,\mathrm{Im}\,G + 2\frac{\partial f(k_0)}{\partial T}\,\mathrm{Re}\,\Sigma\,\mathrm{Im}\,S\bigg] = 0, \tag{13}$$

leading to the remarkably simple formulas [22,23,26]:

$$S = -\mathrm{tr}\int_K \frac{\partial n(k_0)}{\partial T}[\mathrm{Im}\log G^{-1} - \mathrm{Im}\,\Pi\,\mathrm{Re}\,G] - 2\,\mathrm{tr}\int_K \frac{\partial f(k_0)}{\partial T}[\mathrm{Im}\log S^{-1} - \mathrm{Im}\,\Sigma\,\mathrm{Re}\,S], \tag{14}$$

$$\mathcal{N} = -2\,\mathrm{tr}\int_K \frac{\partial f(k_0)}{\partial \mu}[\mathrm{Im}\log S^{-1} - \mathrm{Im}\,\Sigma\,\mathrm{Re}\,S], \tag{15}$$

where we have dropped the label "2-loop" that could be attached to S and $\mathcal{N}$.

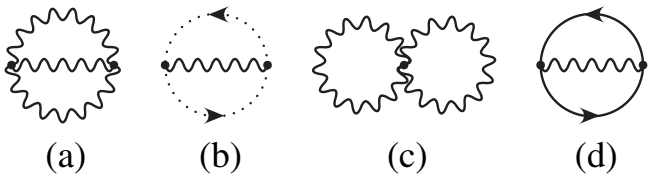

FIG. 1. Diagrams for Φ at 2-loop order in QCD. Wiggly, plain, and dotted lines refer, respectively, to gluons, quarks, and ghosts. Only diagram (d) contributes at next-to-leading order in the large-N_f limit.

Through these formulas, effectively one-loop integrals, all interactions below perturbative order g^4 are summarized by spectral data only, which shows that entropy and density are the preferred quantities for a quasiparticle description. In particular, the term g^3, which usually spoils the apparent convergence of strict perturbative expansions, is now incorporated in a nonpolynomial expression, together with (incompletely resummed) higher-order terms.

Moreover, these expressions are UV finite as soon as the self-energies are, and thus the former are useful as a starting point for further approximations. In Refs. [21–23] it was proposed to use the gauge-invariant hard thermal loops for this purpose. Before considering HTL's, we recall some general properties of self-energies.

B. Bosonic and fermionic self-energies

In the Coulomb gauge, the gauge propagator can be decomposed into a longitudinal and a transverse contribution,

$$G_{00}(K) = G_{\rm L}(K), \qquad G_{ij}(K) = \left\{\delta_{ij} - \frac{k_i k_j}{k^2}\right\} G_{\rm T}(K), \tag{16}$$

and we define corresponding self-energy components through

$$G_{\rm L}(K) = \frac{-1}{k^2 + \Pi_{\rm L}(K)}, \qquad G_{\rm T}(K) = \frac{1}{-K^2 + \Pi_{\rm T}(K)}. \tag{17}$$

Longitudinal and transverse spectral functions are introduced according to

$$\begin{aligned} G_{\rm L}(\omega, k) &= -\frac{1}{k^2} + \int_{k_0} \frac{\rho_{\rm L}(K)}{k_0 - \omega}, \\ G_{\rm T}(\omega, k) &= \int_{k_0} \frac{\rho_{\rm T}(K)}{k_0 - \omega}. \end{aligned} \tag{18}$$

In the following it will be convenient to write the temporal component of the Coulomb gauge propagator alternatively as

$$G_{00}(K) = \frac{k_0^2 - k^2}{k^2} G_\ell(K), \tag{19}$$

and the Dyson equations as

$$\begin{aligned} G_{\rm T}^{-1} &= -k_0^2 + k^2 + \Pi_{t,\rm th} + \Pi_{t,\rm vac}, \\ G_\ell^{-1} &= -k_0^2 + k^2 + \Pi_{\ell,\rm th} + \Pi_{\ell,\rm vac}, \end{aligned} \tag{20}$$

such that $\Pi_{\rm T} = \Pi_{t,\rm th} + \Pi_{t,\rm vac}$ but $\Pi_{\ell,\rm th} + \Pi_{\ell,\rm vac} = -\Pi_{\rm L}(k_0^2 - k^2)/k^2$. Here we have separated off the vacuum ($T, \mu \to 0$) limit of the self-energy components. In the large-N_f limit, we shall have that $\Pi_{t,\rm vac} = \Pi_{\ell,\rm vac} \equiv \Pi_{\rm vac}$ even in the noncovariant Coulomb gauge.

The most general form of the self-energy Σ at finite temperature and density can be written as

$$\Sigma(K) = a(K)\gamma^0 + b(K)\hat{\mathbf{k}} \cdot \boldsymbol{\gamma} + c(K). \tag{21}$$

We define the projection of the self-energy on $\not{K} - M$ as

$$\begin{aligned} \bar{\Sigma}(K) &\equiv \mathrm{tr}[(\not{K} + M)\Sigma(K)] \\ &= 4\omega a(\omega, k) + 4k b(\omega, k) + 4M c(\omega, k). \end{aligned} \tag{22}$$

In the massless case, $c(K) = 0$, and the quark propagator at finite temperature or density can be split into two separate components with opposite ratio of chirality over helicity:

$$\Delta_\pm(K) = \frac{1}{-\omega \pm [k + \Sigma_\pm(K)]}, \tag{23}$$

where

$$\Sigma_\pm(K) \equiv b(K) \pm a(K). \tag{24}$$

Furthermore, $\bar{\Sigma}(K)$ and $\Sigma_\pm(K)$ on the light cone $\omega = \pm k$ are related by

$$\Sigma_\pm(\omega = \pm k, k) = \frac{1}{4k} \bar{\Sigma}(\omega = \pm k, k) \tag{25}$$

(see also Appendix B for a relation between Σ_+ and Σ_-).

C. HTL approximation of the self-consistent entropy

The HTL effective action [15,16] is an effective action for soft modes with energy scales $\sim gT$, which are, at least parametrically, at smaller energy than the hard modes defined by the temperature scale T (or the chemical potential when $\mu \gg T$). At hard scales, the HTL effective action is no longer accurate, except at small virtuality, but this is indeed the phase space domain which contributes the leading-order interaction terms $\propto g^2$ in the expressions (14) and (15). The order g^2 contribution is obtained by expanding out the propagators and keeping a single self-energy insertion. In SU(N) gauge theory with $N_g = N^2 - 1$ gluons and N_f massless quarks this leads to

$$\begin{aligned} S_2 = {} & 2N_g \int_K \frac{\partial n(k_0)}{\partial T} \,\mathrm{Re}\,\Pi_{\rm T}\,\mathrm{Im}\,\frac{1}{k_0^2 - k^2} \\ & + 4NN_f \int_K \frac{\partial f(k_0)}{\partial T} \Big[\mathrm{Re}\,\Sigma_+\,\mathrm{Im}\,\frac{1}{k_0 - k} \\ & - \mathrm{Re}\,\Sigma_-\,\mathrm{Im}\,\frac{1}{k_0 + k} \Big], \end{aligned} \tag{26}$$

and similarly in the density expression. The imaginary part of the free propagator puts the self-energy insertions on the light cone, where they are accurately (to order g^2) given by the HTL value[2] of the transverse component of the gluon self-energy $\Pi_{\rm T}$,

$$\hat{\Pi}_{\rm T}(k_0 = k) = \hat{m}_\infty^2 = \tfrac{1}{2}\hat{m}_D^2, \tag{27}$$

[2]Here and in what follows we shall denote HTL values by putting a hat on the quantities in question.

and the HTL value of $\Sigma_\pm \equiv \frac{1}{2}(\vec{\gamma}\,\vec{k}/|\vec{k}| \pm \gamma_0)\Sigma$,

$$\hat{\Sigma}_{\pm}(k_0 = \pm k) = \frac{\hat{M}_\infty^2}{2k} = \frac{\hat{M}^2}{k}, \tag{28}$$

even though k is no longer soft [42,43]. The leading-order terms in the interaction contribution to the thermodynamic potentials S and $\mathcal{N}$ are thus related to the "asymptotic" thermal masses m_∞ and M_∞ of hard gluons and fermions, respectively. As indicated in Eqs. (27) and (28), at leading order these are proportional to the HTL Debye mass $\hat{m}_D$ and HTL fermionic plasma frequency $\hat{M}$, given by

$$\begin{aligned} \hat{m}_D^2 &= (2N + N_f)\frac{g^2T^2}{6} + N_f\frac{g^2\mu^2}{2\pi^2}, \\ \hat{M}^2 &= \frac{g^2C_f}{8}\left(T^2 + \frac{\mu^2}{\pi^2}\right), \end{aligned} \tag{29}$$

for (uniform) quark chemical potential μ and $C_f = (N^2 - 1)/(2N)$.

However, higher-order contributions in the thermodynamic potential cannot be calculated by expanding out the self-energies in the expressions for the thermodynamic potentials given in Sec. II A as this would lead to infrared divergences in the electrostatic sector. At least the Debye mass that appears in the static propagator needs to be resummed, after which one can calculate systematically up to and including order $g^6\log(g)$. But already the first contribution from the soft sector, the "plasmon term" $\propto g^3$ spoils the apparent convergence of a strict perturbative series.

With the above nonperturbative expressions for entropy and density it is now possible to resum simultaneously the effects of Debye screening and other collective phenomena, such as dynamical screening and Landau damping. At soft momentum scales, these are determined to leading order by the HTL self-energy expressions

$$\begin{aligned} \hat{\Pi}_{\mathrm{L}}(k_0, k) &= \hat{m}_D^2\left[1 - \frac{k_0}{2k}\log\frac{k_0 + k}{k_0 - k}\right], \\ \hat{\Pi}_{\mathrm{T}}(k_0, k) &= \frac{1}{2}\left[\hat{m}_D^2 + \frac{k_0^2 - k^2}{k^2}\hat{\Pi}_{\mathrm{L}}\right], \end{aligned} \tag{30}$$

and

$$\hat{\Sigma}_{\pm}(k_0, k) = \frac{\hat{M}^2}{k}\left[1 - \frac{k_0 \mp k}{2k}\log\frac{k_0 + k}{k_0 - k}\right]. \tag{31}$$

Now Dyson-resumming these self-energies into dressed propagators and inserting them into the entropy formula (14) turns out to account for only a fraction of the plasmon term $\sim g^3$. In the entropy formula (14) the larger part of the plasmon term arises from *hard* momentum scales, namely, from corrections to the leading-order asymptotic masses.

Calculation of the next-to-leading-order corrections to the asymptotic thermal masses (27) and (28) itself requires HTL resummation. However, because they are given by self-energies with a hard external momentum, they involve only a single HTL propagator and no HTL vertices, see Figs. 2 and 3.

FIG. 2. NLO contributions to $\delta\Pi_{\mathrm{T}}$ at hard momentum. Thick dashed and wiggly lines with a blob represent HTL-resummed longitudinal and transverse propagators, respectively. In the large-N_f limit the blobs represent full 1-loop resummed propagators. In this limit, these diagrams are suppressed by a factor of $1/N_f$.

These corrections to the asymptotic thermal masses are, in contrast to their leading-order (HTL) values, nontrivial functions of the momentum,

$$\begin{aligned} \delta m_\infty^2(k) &\equiv \mathrm{Re}\,\delta\Pi_{\mathrm{T}}(k_0 = k), \\ \delta M_\infty^2(k) &\equiv \mathrm{Re}\,2k\delta\Sigma_+(k_0 = k). \end{aligned} \tag{32}$$

At next-to-leading order HTL perturbation theory these expressions can be evaluated only numerically. However, through their contribution to the plasmon term, the following weighted averages are determined to order g^3 and given by remarkably simple results [21–23]:

$$\bar{\delta}m_\infty^2 \equiv \frac{\int dk k\frac{\partial n(k)}{\partial T}\delta m_\infty^2(k)}{\int dk k\frac{\partial n(k)}{\partial T}} = -\frac{1}{2\pi}g^2NT\hat{m}_D + O(g^4), \tag{33}$$

$$\bar{\delta}M_\infty^2 \equiv \frac{\int dk k\frac{\partial f(k)}{\partial T}\delta M_\infty^2(k)}{\int dk k\frac{\partial f(k)}{\partial T}} = -\frac{1}{2\pi}g^2C_fT\hat{m}_D + O(g^4). \tag{34}$$

Note that these results pertain only to the hard excitations; corrections to the various thermal masses of soft excitations are known to differ substantially from (33). For instance, the relative correction to the gluonic plasma frequency [44] at $k = 0$, $\delta m_{pl.}^2/\hat{m}_{pl.}^2$, is only about a third of $\bar{\delta}m_\infty^2/m_\infty^2$; the NLO correction to the non-Abelian Debye mass on the other hand is even positive for small coupling and moreover logarithmically enhanced [45],

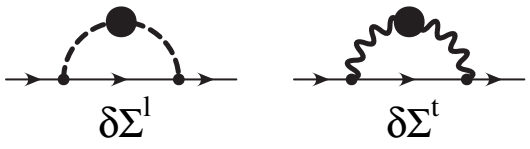

FIG. 3. Same as Fig. 2 for the NLO contributions to $\delta\Sigma$ at hard momentum. Although in the large-N_f limit these diagrams are also suppressed individually by a factor of N_f, they nevertheless contribute to the entropy at order N_f^0.

$$\delta m_D^2 = +\frac{1}{2\pi} g^2 N T \hat{m}_D \log\frac{c}{g}, \tag{35}$$

where the constant under the logarithm is nonperturbative and cannot be calculated by weak-coupling techniques. However these corrections to the dispersion laws at soft momenta lead to contributions to the thermodynamic potential which are beyond the perturbative accuracy of the two-loop functionals (14) and (15), and thus we do not include them in our definition of next-to-leading-order HTL approximation of the entropy or density. This we instead define as an evaluation of (14) and (15) with HTL propagators and self-energies, which at hard momenta include the complete corrections to the asymptotic thermal masses (32). In Refs. [21–23,36] only the averaged next-to-leading order asymptotic masses (33) and (34) were taken into account.

In this paper we shall evaluate the complete momentum dependence of the next-to-leading order asymptotic quark masses $\delta M_\infty^2(\mathrm{k})$, which is the only correction also relevant at large N_f. While both (33) and (34) are suppressed by $1/N_f$ in the large-N_f limit, the latter eventually gets multiplied by a factor N_f. We then compare with the exact nonperturbative results that one can derive in the large-N_f limit [33–35].

III. LARGE-N_f EXPANSION OF THE THERMODYNAMIC POTENTIAL

We shall now focus on the large-N_f limit of the thermodynamic potential, which is nonperturbative in the effective coupling constant and therefore requires nonperturbative renormalization. In this respect we extend the previous derivations of Ref. [33–35] to include nonzero quark masses (see also [46]), even though the final numerical evaluation will be carried out only for the massless case. We then discuss the special features of the self-consistent entropy and density expressions in the large-N_f limit.

A. Large-N_f limit of the 2PI thermodynamic potential

The thermodynamic potential of Eq. (8) is given in terms of full propagators G and S and the Φ functional, the sum of all 2PI diagrams. In the large-N_f limit, the Φ functional reduces to a single two-loop skeleton diagram, namely, the last one of those displayed in Fig. 1. Only this diagram remains of order 1 when $g^2 \to 0, N_f \to \infty$ with fixed $g_{\rm eff}^2 \propto g^2 N_f \sim O(1)$. Furthermore, the fermion propagator in this diagram can be replaced by the free one, since a fermion self-energy is of order $\Sigma \sim 1/N_f$. Hence,

$$\Phi[G, S] \to \Phi_*[G] = \tfrac{1}{2}\mathrm{Tr}(\Pi_* G) \tag{36}$$

where Π_* is a fermion bubble involving the free fermion propagator S_0, and is proportional to $g_{\rm eff}^2$. From a variational point of view, Π_* is now a fixed quantity, and the self-consistent Π defined through Eq. (11) is equal to it because $\Phi_*[G]$ is linear in G. Hence, $\Pi = 2\delta\Phi_*[G]/\delta G = \Pi_*$. On the other hand, $S = S_0$ is no longer a variational quantity at all. We thus have

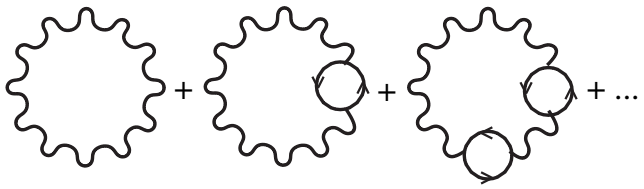

FIG. 4. Fermion bubble resummation contributing to the pressure to next-to-leading order in the $1/N_f$ expansion.

$$\Omega[G, S] \to \Omega_*[G] = -T\,\mathrm{Tr}\log S_0^{-1} + \tfrac{1}{2}T\,\mathrm{Tr}\log G^{-1} - \tfrac{1}{2}T\,\mathrm{Tr}(\Pi G) + \Phi_*[G], \tag{37}$$

which, when evaluated at its extremal point and setting $G_*^{-1} = G_0^{-1} + \Pi_*$, reduces to[3]

$$\Omega_*[G_*] = -PV = -T\,\mathrm{Tr}\log S_0^{-1} + \tfrac{1}{2}T\,\mathrm{Tr}\log G_*^{-1}. \tag{38}$$

Diagrammatically, the pressure at leading order (N_f^1) is thus just given by the free fermion loop. It contains an overall, temperature-independent divergence which can be eliminated by subtracting the corresponding vacuum pressure:

$$P_0^f = N N_f\,\mathrm{tr}\Big[\sum\!\!\!\!\!\!\int_K \log S_0^{-1} - \int_{K_{\rm E}} \log S_0^{-1}\Big]. \tag{39}$$

In Eq. (39) and in the rest of this section (III A), we perform explicitly flavor and color traces. Thus the symbol ''tr'' only denotes a trace over spin indices. The next-to-leading order contribution $\sim N_f^0$ is obtained from the resummation of the bosonic self-energy Π (see Fig. 4) on the gluon propagator (ring resummation):

$$\Pi_{\rm b}^{\mu\nu}(Q) = g_{\rm eff}^2\,\mathrm{tr}\sum\!\!\!\!\!\!\int_K \gamma^\mu S_0(K)\gamma^\nu S_0(K-Q), \tag{40}$$

which one can split into a vacuum and a thermal piece (see Appendix A 1):

$$\Pi_{\rm b,vac}^{\mu\nu}(Q) = g_{\rm eff}^2\,\mathrm{tr}\int_{K_{\rm E}} \gamma^\mu S_0(K)\gamma^\nu S_0(K-Q),$$
$$\Pi_{\rm th}^{\mu\nu}(Q) = -2g_{\rm eff}^2\,\mathrm{tr}\int_K \gamma^\mu(\not{K}+M)\sigma_0(K)\gamma^\nu S_0(K-Q), \tag{41}$$

with $\sigma_0(K) = \epsilon(k_0) f(|k_0|)\rho_0(K)$.

This function $\sigma_0(K)$ is a particular combination of the thermal factor and the spectral density which appears systematically when isolating thermal contributions in

[3]We stress here that viewed as a functional of $G_* \to G$, the right-hand side of Eq. (38) is not stationary at $G_*^{-1} = G_0^{-1} + \Pi_*$ and thus one cannot use the same simplifications to compute the entropy as in the 2PI framework. In order to do so, one should rather work with Eq. (37).

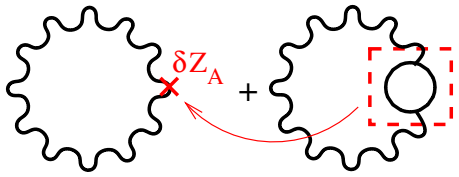

FIG. 5 (color online). Role of the counterterm δZ_A: every time that a fermion bubble is inserted, one has to insert the corresponding counterterm δZ_A to absorb the subdivergence.

the Matsubara formalism [47]. The thermal factor $f(|k_0|)$ only involves positive energies and thus the thermal contribution is UV finite. We will also need the dominant UV asymptotic behavior of $\Pi^{\mu\nu}_{\rm th}$. Since the momentum K is cut off by the temperature, the leading asymptotic behavior at large Q is *a priori* determined by $S_0(K-Q) \sim 1/Q$. However, since the gluon self-energy is an even function of Q, this asymptotic behavior is in fact improved to $1/Q^2$.[4]

The vacuum piece $\Pi^{\mu\nu}_{\rm b,vac}$ is UV divergent (hence the label "b" standing for "bare"). However, to the same order in N_f, one can add the counterterm $\delta Z_A\{Q^2 g^{\mu\nu} - Q^\mu Q^\nu\}$, with δZ_A adjusted in order to absorb the divergence. The UV finite self-energy then reads

$$\Pi^{\mu\nu}_{\rm vac}(Q) = g^2_{\rm eff}\,{\rm tr}\int_{K_{\rm E}} \gamma^\mu S_0(K)\gamma^\nu S_0(K-Q) + \delta Z_A\{Q^2 g^{\mu\nu} - Q^\mu Q^\nu\}. \tag{42}$$

The role of δZ_A in the ring resummation is illustrated in Fig. 5. In general, the ring resummation does not account for all the next-to-leading order contributions. Indeed, the fermionic mass and field strength counterterms (δM and δZ_ψ) are of order $1/N_f$, and can be inserted in a fermion loop (see Fig. 6) to generate a contribution of order N_f^0. This contribution is needed to remove potential subdivergences as illustrated in Fig. 7.

Once all subdivergences are eliminated, there remains an overall, temperature-independent divergence in the pressure, which can be eliminated by subtracting the vacuum pressure at next-to-leading order:

$$P - P_0^f = NN_f\,{\rm tr}\Big[\sum\!\!\!\!\!\!\int_K (\delta M - \not{K}\delta Z_\psi)S_0 - \int_{K_{\rm E}} (\delta M - \not{K}\delta Z_\psi)S_0\Big] - \frac{N_g}{2}\,{\rm tr}\Big[\sum\!\!\!\!\!\!\int_Q \log(G_0^{-1}+\Pi) - \int_{Q_{\rm E}} \log(G_0^{-1}+\Pi_{\rm vac})\Big]. \tag{43}$$

It is perhaps surprising that the first line of this formula did not appear in the general derivation given at the beginning of this section. This is because the derivation there was made using bare quantities. If one rewrites Eq. (38) in terms of renormalized quantities, one generates these extra terms. Performing the Matsubara sums in Eq. (43), one obtains

$$\begin{aligned} P - P_0^f = {} & -NN_f\,{\rm tr}\int_K (\delta M - \not{K}\delta Z_\psi)(\not{K} + M)\sigma_0(K) \\ & - N_g\,{\rm tr}\int_Q \epsilon(q_0)n(|q_0|)\,{\rm Im}\log(G_0^{-1}+\Pi) \\ & - \frac{N_g}{2}\,{\rm tr}\int_{Q_{\rm E}} [\log(G_0^{-1}+\Pi) \\ & - \log(G_0^{-1}+\Pi_{\rm vac})]. \end{aligned} \tag{44}$$

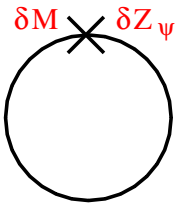

FIG. 6 (color online). Fermion "counterterms" eliminating next-to-leading order divergences in the bubble resummation of Fig. 4.

The pressure in Eq. (44) contains a contribution carrying the counterterms, a second contribution which is explicitly finite due to the presence of the factor $n(|q_0|)$, and a potentially divergent part which reads ($A \simeq B$ here means that the divergent parts of A and B coincide)

$$(P - P_0^f)^{\rm div} \simeq -\frac{N_g}{2}\,{\rm tr}\int_{Q_{\rm E}} [\log(G_0^{-1}+\Pi) - \log(G_0^{-1}+\Pi_{\rm vac})], \tag{45}$$

or, after performing the traces explicitly (see also [34]),

$$(P - P_0^f)^{\rm div} \simeq -N_g \int_{Q_{\rm E}}\Big[\log\Big(1 + \frac{\Pi_{t,{\rm th}}}{-Q^2+\Pi_{\rm vac}}\Big) - \frac{1}{2}\log\Big(1 + \frac{\Pi_{\ell,{\rm th}}}{-Q^2+\Pi_{\rm vac}}\Big)\Big]. \tag{46}$$

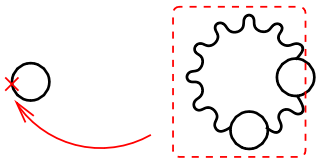

FIG. 7 (color online). Potential singularity with the structure of a fermion self-energy insertion. It appears when one of the fermionic momenta is kept fixed while all others momenta are taken to infinity. The structure of the diagram needed to absorb this potential singularity is exactly that of the diagram in Fig. 6.

[4] A more detailed analysis of the asymptotic behavior can be found in the appendix of Ref. [33].

Using the asymptotic behavior of $\Pi_{t,\mathrm{th}}$ and $\Pi_{\ell,\mathrm{th}}$ which can be found in the appendix of Ref. [33], one can show that the potential divergent term arises from the leading terms in the expansion of the logarithms:

$$(P - P_0^f)^{\mathrm{div}} \simeq -\frac{N_g}{2}\int_{Q_\mathrm{E}} \frac{\Pi_{\ell,\mathrm{th}} + 2\Pi_{t,\mathrm{th}}}{-Q^2 + \Pi_{\mathrm{vac}}} = -\frac{N_g}{2}\int_{Q_\mathrm{E}} \Pi_{\mathrm{th}}^{\mu\nu} G_{\mu\nu}^{\mathrm{vac}}, \tag{47}$$

or using the expression (41) for $\Pi_{\mathrm{th}}^{\mu\nu}$ and $C_f = N_g/(2N)$,

$$(P - P_0^f)^{\mathrm{div}} \simeq NN_f\,\mathrm{tr}\int_K (\not{K} + M)\sigma_0(K) \times\left[g^2 C_f \int_{Q_\mathrm{E}} \gamma^\nu S_0(K-Q)\gamma^\mu G_{\mu\nu}^{\mathrm{vac}}(Q)\right]. \tag{48}$$

As we shall see in Sec. IV B, in the process of performing the analytic continuation in k_0 of the quantity in brackets in the formula above, one has to deform the contour of the Q_E integration in order to avoid crossing singularities. However, here we are only interested in the UV contributions. Since contour deformation will only be necessary for $Q_E \leq 2k = 2k_0$ as we will see at the end of Sec. IV B 1, we can identify the integral over Q_E with the vacuum fermion self-energy [see Eq. (69) below], and write

$$(P - P_0^f)^{\mathrm{div}} \simeq -NN_f\,\mathrm{tr}\int_K (\not{K} + M)\sigma_0(K)\Sigma_{\mathrm{b,vac}}[G_{\mathrm{vac}}](K). \tag{49}$$

We now add this divergent contribution to that of the counterterms δM and δZ_ψ and get

$$(P - P_0^f)^{\mathrm{ct+div}} \simeq -NN_f\,\mathrm{tr}\int_K (\not{K} + M)\sigma_0(K)[\delta M - \not{K}\delta Z_\psi + \Sigma_{\mathrm{b,vac}}[G_{\mathrm{vac}}](K)], \tag{50}$$

which can be made finite by a suitable adjustment of δM and δZ_ψ.

In the massless case the divergences associated with the fermionic self-energies do not contribute to the pressure. As M vanishes, and $\not{K} = 0$, it is clear that δM does not contribute. One can verify that δZ_ψ does not contribute in two ways. From (50) we have

$$(P - P_0^f)^{\mathrm{ct}} \longrightarrow NN_f\delta Z_\psi\,\mathrm{tr}\int_K \not{K}\sigma_0(K)\not{K} = 2\pi NN_f\delta Z_\psi\,\mathrm{tr}\int_K f(|k_0|)\delta(K^2)K^2 = 0. \tag{51}$$

Equivalently, one can rewrite the potentially divergent piece as

$$(P - P_0^f)^{\mathrm{div}} \longrightarrow NN_f\,\mathrm{tr}\int_K \not{K}\sigma_0(K)\Sigma_{\mathrm{b,vac}}[G_{\mathrm{vac}}](K) = 2\pi NN_f\int_K f(|k_0|)\delta(K^2)\bar{\Sigma}_{\mathrm{vac}}[G_{\mathrm{vac}}](K). \tag{52}$$

As we shall explain in Sec. IV C, $\bar{\Sigma}_{\mathrm{vac}}[G_{\mathrm{vac}}] \equiv \mathrm{tr}(\not{K}\Sigma_{\mathrm{vac}}[G_{\mathrm{vac}}])$ vanishes on the light cone. This result is in one-to-one correspondence with the fact that, in the massless case, the large-Q contribution of the integrand in (47) vanishes after integration over Q [33,34]. This is due to the vanishing of the angular integral and requires that numerical computations use a cutoff respecting Euclidean symmetry. Although we shall eventually work with renormalized quantities obtained in the symmetry-preserving dimensional regularization, the numerical evaluations require a cutoff to eliminate the Landau pole of the large-N_f theory. As we shall discuss further in Sec. IV, if this cutoff does not respect Euclidean rotation invariance, it leads to spurious contributions.

With renormalized self-energy Π, Eq. (44) reduces in the massless case to [33–35]

$$P - P_0^f = -\frac{N_g}{2}\,\mathrm{tr}\Big[\sum\!\!\!\!\!\!\int_Q \log(G_0^{-1} + \Pi) - \int_{Q_\mathrm{E}} \log(G_0^{-1} + \Pi_{\mathrm{vac}})\Big]. \tag{53}$$

B. Large-N_f limit of the self-consistent entropy

The entropy could be obtained by taking a total derivative of the pressure with respect to the temperature. Using Eq. (53) for the pressure, this leads to

$$S - S_0 = \frac{d(P - P_0)}{dT} = -\mathrm{tr}\int_K \frac{\partial n(k_0)}{\partial T}\,\mathrm{Im}\log(G^{-1}G_0) - \mathrm{tr}\int_K n(k_0)\,\mathrm{Im}\Big(G\frac{d\Pi_*}{dT}\Big) \tag{54}$$

where $G^{-1} = G_0^{-1} + \Pi_*$ and we subtracted the fermionic and the bosonic interaction-free contributions to the pressure $P_0 = P_0^f + P_0^b$. Note that the overall temperature-independent divergence that is present in the pressure disappears when considering the entropy. As we shall see, the only remaining divergences are associated with the self-energies. This is, however, not manifest in Eq. (54), where the second term is potentially divergent for $k_0 \to -\infty$.

Using that $\Phi_*[G]$ is a two-loop diagram for which S' as defined in Eq. (13) vanishes identically, we have

$$\frac{\partial(T\Phi_*[G])}{\partial T}\bigg|_G = \mathrm{tr}\int_K\Big[\frac{\partial n(k_0)}{\partial T}\,\mathrm{Re}\,\Pi_*\,\mathrm{Im}\,G + 2\frac{\partial f(k_0)}{\partial T}\,\mathrm{Re}\,\Sigma\,\mathrm{Im}\,S_0\Big], \tag{55}$$

where Σ is the $O(N_f^{-1})$ fermionic self-energy obtained by calculating the one-loop diagram composed of a bare

fermion propagator and a full large-N_f gauge boson propagator (see Sec. IV).

On the other hand,

$$\frac{\partial(T\Phi_*[G])}{\partial T}\bigg|_G = \frac{\partial}{\partial T}\left(\frac{T}{2}\,\mathrm{Tr}(\Pi_* G)\right)\bigg|_G = \frac{\partial}{\partial T}\left(\mathrm{tr}\int_K n(k_0)\,\mathrm{Im}(\Pi_* G)\right)\bigg|_G = \mathrm{tr}\int_K \frac{\partial n(k_0)}{\partial T}\,\mathrm{Im}(\Pi_* G) + \mathrm{tr}\int_K n(k_0)\,\mathrm{Im}\left(G\frac{d\Pi_*}{dT}\right). \tag{56}$$

Combining Eqs. (54)–(56) yields

$$S - S_0 = -\mathrm{tr}\int_K \frac{\partial n(k_0)}{\partial T}[\mathrm{Im}\log(G^{-1}G_0) - \mathrm{Im}\,\Pi\,\mathrm{Re}\,G] - 2\,\mathrm{tr}\int_K \frac{\partial f(k_0)}{\partial T}\,\mathrm{Re}\,\Sigma\,\mathrm{Im}\,S_0, \tag{57}$$

where S_0 denotes the ideal-gas limit of the entropy.

This expression can in fact be derived also from the 2-loop-Φ-derivable expression for the entropy, Eq. (14). In the large-N_f limit, the full gauge boson self-energy Π reduces to the fermion loop involving undressed propagators. Any fermion self-energy diagram insertion (Fig. 3) in Π would bring in a factor g^2 without a factor N_f, leading to a subleading correction. However, one fermion self-energy has to be included in $\mathrm{tr}\log S^{-1} = \mathrm{tr}\log(S_0^{-1} + \Sigma)$ in order to produce contributions of order N_f^1 and N_f^0. The integrand of the fermionic terms in the 2-loop entropy and density, Eqs. (14) and (15), therefore simplifies according to

$$\mathrm{Im}\,\log S^{-1} - \mathrm{Im}\,\Sigma\,\mathrm{Re}\,S \to \mathrm{Im}\log S_0^{-1} + \mathrm{Im}(\Sigma S_0) - \mathrm{Im}\,\Sigma\,\mathrm{Re}\,S_0 + O(N_f^{-1}) \to \mathrm{Im}\log S_0^{-1} + \mathrm{Re}\,\Sigma\,\mathrm{Im}\,S_0. \tag{58}$$

This enables us to recover Eq. (57) for the entropy, while we get

$$\mathcal{N} - \mathcal{N}_0 = -2\,\mathrm{tr}\int_K \frac{\partial f(k_0)}{\partial \mu}\,\mathrm{Re}\,\Sigma\,\mathrm{Im}\,S_0 \tag{59}$$

for the contribution of order N_f^0 to the density.

In contrast to Eq. (54), Eq. (57) is a manifestly ultraviolet finite expression as soon as propagators and self-energies are made finite through renormalization, and it naturally identifies bosonic and fermionic quasiparticle entropies, $S = S_b + S_f$, with vanishing residual interactions S'.

C. HTL approximation of the large-N_f entropy

In the large-N_f limit, the two expressions for the entropy, Eqs. (54) and (57), are completely equivalent. However, this equivalence is broken once one starts approximating the gluon self-energy Π_* by its HTL limit which has different behavior at large momentum. Doing so leads to uncanceled UV divergences in Eq. (54), whereas the entropy formula (57) that was derived using the stationarity of the thermodynamic potential for self-consistent solutions remains finite. In the following we shall investigate the quantitative difference it makes to approximate the full large-N_f gluon self-energy by its HTL approximation and define

$$\hat{S} = S_0 - \mathrm{tr}\int_K \frac{\partial n(k_0)}{\partial T}[\mathrm{Im}\log(\hat{G}^{-1}G_0) - \mathrm{Im}\,\hat{\Pi}\,\mathrm{Re}\,\hat{G}] - 2\,\mathrm{tr}\int_K \frac{\partial f(k_0)}{\partial T}\,\mathrm{Re}\,\Sigma[\hat{G}]\,\mathrm{Im}\,S_0 = S_0 + \hat{S}_b + \hat{S}_f, \tag{60}$$

where $\hat{\Pi}$ and $\hat{G}$ denote the gluon HTL self-energy and propagator, respectively. The numerical evaluation of this expression does not contain spurious divergences, because $\mathrm{Re}\,\Sigma[\hat{G}]$ on the light cone is UV finite as we will show in Sec. IV C. This is the advantage of using the self-consistent 2PI formulation rather than a direct ring resummation.

It is in fact instructive to evaluate the difference between Eq. (60) and a direct HTL approximation of $d(P - P_0)/dT$ as given by Eq. (54). In the large-N_f limit the equivalence of the two entropy formula stems from Eqs. (55) and (56) which combine together into

$$\mathrm{tr}\int_K \frac{\partial n(k_0)}{\partial T}\,\mathrm{Im}\,\Pi_*\,\mathrm{Re}\,G - 2\,\mathrm{tr}\int_K \frac{\partial f(k_0)}{\partial T}\,\mathrm{Re}\,\Sigma\,\mathrm{Im}\,S_0 = -\mathrm{tr}\int_K n(k_0)\,\mathrm{Im}\left(G\frac{d\Pi_*}{dT}\right). \tag{61}$$

In the HTL approximation, it is possible to derive a similar formula by exploiting the fact that Eqs. (55) and (56) are valid for any G provided one maintains the functional relation of Σ to G. The value of Π_* does not need to be changed. Thus, if we replace $G \to \hat{G}$, $\Sigma \to \Sigma[\hat{G}]$, we obtain

$$\mathrm{tr}\int_K \frac{\partial n(k_0)}{\partial T}\,\mathrm{Im}\,\Pi_*\,\mathrm{Re}\,\hat{G} - 2\,\mathrm{tr}\int_K \frac{\partial f(k_0)}{\partial T}\,\mathrm{Re}\,\Sigma[\hat{G}]\,\mathrm{Im}\,S_0 = -\mathrm{tr}\int_K n(k_0)\,\mathrm{Im}\left(\hat{G}\frac{d\Pi_*}{dT}\right). \tag{62}$$

Now we add a common term to both sides in order to obtain the 2PI HTL entropy in the form:

$$\hat{S} = \frac{d}{dT}((P - P_0^f)|_{\Pi_*\to\hat{\Pi}}) + \mathrm{tr}\int_K \frac{\partial n(k_0)}{\partial T}\,\mathrm{Im}(\hat{\Pi} - \Pi_*)\,\mathrm{Re}\,\hat{G} + \mathrm{tr}\int_K n(k_0)\,\mathrm{Im}\left[\hat{G}\left(\frac{d\hat{\Pi}}{dT} - \frac{d\Pi_*}{dT}\right)\right]. \tag{63}$$

The last two terms are the ones corresponding to the

temperature dependent singularities in a direct HTL approximation on ring diagrams.

Returning to the expression (60), we observe that the large-N_f limit leads to rather different simplifications in the bosonic and the fermionic contributions. In the bosonic part $\hat{S}_b$, the NLO contributions $\delta\Pi$ displayed in Fig. 2 do not appear because they are of order N_f^{-1}. The NLO contribution $\delta\Sigma$ of Fig. 3 is also of order N_f^{-1}, but it does contribute to the fermionic entropy because there are N_f fermions. However, $\delta\Sigma$ is not Dyson-resummed because for $N_f \to \infty$ only one insertion of $\delta\Sigma$ survives.

Because of the factor $\mathrm{Im}\, S_0$, the fermion self-energy in (57) and (60) is evaluated on mass shell and, because the integral is dominated by hard momenta, the fermionic contribution to the entropy can be identified with a weighted average over a momentum-dependent asymptotic quark mass. For the entropy[5] at zero chemical potential, we can define

$$(S - S_0)_f = -2\,\mathrm{tr}\int_K \frac{\partial f(k_0)}{\partial T}\,\mathrm{Re}\,\Sigma\,\mathrm{Im}\,S_0 = -4NN_f\int_{\mathbf{k}}\frac{\partial f(k)}{\partial T}\,\frac{M_\infty^2(k)}{2k} \equiv -\frac{NN_fT}{6}\bar{M}_\infty^2, \tag{64}$$

although, as we shall see, $M_\infty^2(k)$ and $\bar{M}_\infty^2$ do not need to be positive.

In perturbation theory we have in the massless case and at zero chemical potential

$$N_f\bar{M}_\infty^2 = \left[\frac{g_{\mathrm{eff}}^2}{2} - \frac{g_{\mathrm{eff}}^3}{\sqrt{3}\pi} + O(g_{\mathrm{eff}}^4)\right]C_fT^2, \qquad C_f = \frac{N_g}{2N}, \tag{65}$$

where the calculation of the contribution $\propto g^3$ requires HTL resummation as shown in Fig. 3. The latter is responsible for $3/4$ of the plasmon term in the thermodynamic potential; the remaining $1/4$ of the plasmon term comes from the soft momentum regime of the bosonic entropy (57).

In the following we shall derive and evaluate numerically the quantities $M_\infty^2(k)$ and $\bar{M}_\infty^2$ in the large-N_f limit. These will be compared with strictly perturbative results and HTL approximations where all the higher-order terms generated by HTL resummation are retained. This will allow us to test the proposal of complete HTL resummation not only with respect to the entropy of large-N_f QCD but also with respect to the asymptotic thermal quark masses.

IV. FERMION SELF-ENERGY

In this section we shall calculate the fermionic self-energy Σ in the large-N_f limit as it is needed in the self-consistent entropy and number density formula Eqs. (57) and (59). It corresponds to the one-loop diagram of Fig. 3 with an undressed fermion line and a dressed gluon propagator which resums the fermion bubbles in analogy to Fig. 4. The fermion self-energy requires mass and wave function renormalization: $\Sigma(K) = \Sigma_{\mathrm{b}}(K) + \delta M - \not{K}\delta Z_\psi$ with the bare self-energy Σ_{b} given by

$$\Sigma_{\mathrm{b}}(K) = -g^2C_f\sum\!\!\!\!\!\!\int_Q \gamma^\mu S_0(K-Q)\gamma^\nu G_{\mu\nu}(Q). \tag{66}$$

It enters the fermionic contribution to the entropy in the second line of Eq. (57) as

$$S^f - S_0^f = -NN_f\int_{\mathbf{k}}\frac{1}{2\varepsilon_k}\left[\frac{\partial f(\varepsilon_k)}{\partial T}\,\mathrm{Re}\,\bar{\Sigma}(\varepsilon_k,k) - \frac{\partial f(-\varepsilon_k)}{\partial T}\,\mathrm{Re}\,\bar{\Sigma}(-\varepsilon_k,k)\right], \tag{67}$$

with $\bar{\Sigma}(K)$ from Eq. (22). In the massless case this reduces to (see Appendix B)

$$S^f - S_0^f = -NN_f\int_{\mathbf{k}}\frac{1}{k}\,\frac{\partial f(k)}{\partial T}\,\mathrm{Re}\,\bar{\Sigma}(k_0 = k, k). \tag{68}$$

We note here that the frequency carried by K in Eq. (66) is imaginary (Matsubara frequency). In contrast the evaluation of the entropy needs the discontinuity of the fermion self-energy across the real axis. The analytical continuation of (66) is described in detail in Sec. IV B. To that purpose, it is convenient to split the self-energy into a vacuum and a thermal piece $\bar{\Sigma}_{\mathrm{b}} = \bar{\Sigma}_{\mathrm{b,vac}} + \bar{\Sigma}_{\mathrm{th}}$ with respect to the overall loop momentum Q. The thermal piece is finite and its analytical continuation causes no troubles (see Sec. IV A). In contrast, the correct evaluation of the vacuum part with respect to the integral over Q needs that we maintain Euclidean invariance (see Sec. IV B). We thus compute it by replacing the discrete sum in (66) by a continuous integral, leading to a 4-dimensional Euclidean integral:

$$\Sigma_{\mathrm{b,vac}}(K) = -g^2C_f\int_{Q_{\mathrm{E}}}\gamma^\mu S_0(K-Q)\gamma^\nu G_{\mu\nu}(Q). \tag{69}$$

This contribution also carries temperature dependences, but only through the gluon propagator. It contains UV divergences which in the massless case disappear from the entropy formula as it is clear by looking at the contribution of the counterterms (once again the trace is performed over the Lorentz group):

$$\mathrm{Re}\,\bar{\Sigma}^{\mathrm{ct}}(\pm\varepsilon_k,k) = \mathrm{Re}\,\mathrm{tr}[(\not{K}+M)(\delta M - \not{K}\delta Z_\psi)]_{k_0=\pm\varepsilon_k} = 4M\delta M - 4M^2\delta Z_\psi. \tag{70}$$

In Sec. IV C, we give a direct proof of the finiteness of $\mathrm{Re}\,\bar{\Sigma}_{\mathrm{b,vac}}$. In what follows, we drop the label "b" on the projected self-energy which reads

[5]For the quark density a different weighted average would be relevant.

$$\bar{\Sigma}(K) = \mathrm{tr}[\not{K}\Sigma(K)]$$
$$= -g^2 C_f \oint\!\!\!\!\!\!\sum_Q \mathrm{tr}[\not{K}\gamma^\mu \not{P}\gamma^\nu]\Delta_0(P)G_{\mu\nu}(Q), \quad (71)$$
$$P = K - Q.$$

Evaluating the trace over γ matrices, one obtains

$$\bar{\Sigma}(K) = -4g^2 C_f \oint\!\!\!\!\!\!\sum_Q [K^\mu P^\nu + P^\mu K^\nu - K\cdot P g^{\mu\nu}]\Delta_0(P)G_{\mu\nu}(Q). \quad (72)$$

In order to pursue the calculation, we need to specify a gauge. We shall use the Coulomb gauge from Sec. II B. By plugging $G_{\mu\nu}(Q)$ from Eq. (16) into Eq. (72), we obtain two components to $\bar{\Sigma}$:

$$\bar{\Sigma}_{\mathrm{L}}(K) = -4g^2 C_f \oint\!\!\!\!\!\!\sum_Q [k_0 p_0 + \mathbf{k}\cdot\mathbf{p}]\Delta_0(P)G_{\mathrm{L}}(Q),$$
$$\bar{\Sigma}_{\mathrm{T}}(K) = -8g^2 C_f \oint\!\!\!\!\!\!\sum_Q [k_0 p_0 - (\hat{\mathbf{q}}\cdot\mathbf{k})(\mathbf{p}\cdot\hat{\mathbf{q}})]\Delta_0(P)G_{\mathrm{T}}(Q), \quad (73)$$

where k_0, q_0 and p_0 are evaluated at the Matsubara frequencies $k_0 = i\omega$, $q_0 = i\omega_n$ and $p_0 = i\omega_m = i\omega - i\omega_n$.

A. Matsubara sums and thermal contributions

The contributions to $\bar{\Sigma}$ that we labeled as "thermal" are those which after performing the Matsubara sum in (73) contain a thermal factor $n(|p_0|)$ or $f(|p_0|)$ which vanishes when $T \to 0$. Note that these contributions do not account for the complete temperature dependences of $\bar{\Sigma}$, since part of the latter is implicit in the dressed gluon propagator. The Matsubara sums are performed in Appendix A 2. The result is

$$\bar{\Sigma}_{\mathrm{L,th}}(K) = 4g^2 C_f \int_P [k_0 p_0 + \mathbf{k}\cdot\mathbf{p}]\sigma_0(P)G_{\mathrm{L}}(K-P) - 4g^2 C_f \int_Q [k_0(k_0 - q_0) + \mathbf{k}\cdot\mathbf{p}] \times \Delta_0(K-Q)\sigma_{\mathrm{L}}(Q), \quad (74)$$

$$\bar{\Sigma}_{\mathrm{T,th}}(K) = 8g^2 C_f \int_P [k_0 p_0 - (\hat{\mathbf{q}}\cdot\mathbf{k})(\mathbf{p}\cdot\hat{\mathbf{q}})] \times \sigma_0(P)G_{\mathrm{T}}(K-P) - 8g^2 C_f \int_Q [k_0(k_0 - q_0) - (\hat{\mathbf{q}}\cdot\mathbf{k})(\mathbf{p}\cdot\hat{\mathbf{q}})]\Delta_0(K-Q)\sigma_{\mathrm{T}}(Q), \quad (75)$$

with $\sigma_0(P) = \epsilon(p_0)f(|p_0|)\rho_0(P)$ and $\sigma_{\mathrm{L,T}}(Q) = \epsilon(q_0)n(|q_0|)\rho_{\mathrm{L,T}}(Q)$ and $K^\mu = (i\omega_l, \mathbf{k})$. These integrals are UV finite thanks to the presence of the thermal factors. The continuation to the real axis $k_0 = i\omega_l \to k_0 = \omega + i\epsilon$ and the light-cone limit $\omega \to k$ pose no problems, since the integrand is always well defined. After performing the angular integrals analytically, one can perform the remaining 2-dimensional integrals numerically.

Since integrations in $\bar{\Sigma}_{\mathrm{th}}$ are effectively cut off by the temperature, the necessity of introducing an ultraviolet cutoff below the scale of the Landau pole is no practical problem for temperatures $T \ll \Lambda_L$. The results will be independent on how such a cutoff is introduced. However, this will be different for the remaining "vacuum" contributions.

B. Vacuum contributions and renormalization

The remaining contributions $\bar{\Sigma}_{\mathrm{vac}}$, which contain temperature dependences (only) through the spectral data of the gluon propagator, can be computed by replacing the discrete sum in (73) by a continuous integral, yielding a 4-dimensional Euclidean integral:

$$\bar{\Sigma}^{\mathrm{vac}}_{\mathrm{L}}(K) = -4g^2 C_f \int_{Q_{\mathrm{E}}} [k_0 p_0 + \mathbf{k}\cdot\mathbf{p}]\Delta_0(P)G_{\mathrm{L}}(Q),$$
$$\bar{\Sigma}^{\mathrm{vac}}_{\mathrm{T}}(K) = -8g^2 C_f \int_{Q_{\mathrm{E}}} [k_0 p_0 - (\hat{\mathbf{q}}\cdot\mathbf{k})(\mathbf{p}\cdot\hat{\mathbf{q}})]\Delta_0(P)G_{\mathrm{T}}(Q), \quad (76)$$

where $K = (k_0, k) = (i\omega_l, \mathbf{k})$, $P = (p_0, \mathbf{p}) = (i\omega_m, p)$, and $Q = (q_0, q) = (i\omega_n, q)$ have imaginary frequency to start with, and $P + Q = K$. Since our theory contains a Landau pole, we have to introduce a cutoff below that scale, and it is important that this cutoff is implemented in a Euclidean-invariant way even when the result would be finite in dimensional regularization.

1. Cutoff implementation example

To give an example of difficulties encountered with a non-Euclidean-invariant cutoff, consider the expression $J(K) = I(K) - I(0)$ with

$$I(K) \equiv \int_{Q_{\mathrm{E}}} \frac{1}{(Q-K)^2}. \quad (77)$$

This quantity appears in the calculation of $\bar{\Sigma}_{\mathrm{vac}}[G_0](K)$ and we would like to evaluate it on the light cone $K^2 = 0$. In dimensional regularization one can shift the integration momentum, and the result is $[I(K) - I(0)] \to [I(0) - I(0)] = 0$ for arbitrary Euclidean momentum K. Hence, the light-cone value of J is zero. Is it possible to recover this result by using an explicit cutoff?

Let us first introduce a cutoff that violates Euclidean invariance: a cutoff that only applies to three-dimensional momenta, not to the frequency (note that we assume imaginary values for q_0 and k_0 such that the integrand does not contain any poles along the integration path):

$$I(K) = \frac{2\pi}{(2\pi)^4}\int_{-i\infty}^{i\infty}\frac{dq_0}{i}\int_0^\Lambda dq\int_{-1}^{1} d(\cos\theta) \times \frac{q^2}{(q_0 - k_0)^2 - (q^2 + k^2 - 2qk\cos\theta)} = -\frac{1}{8\pi^2}\Lambda^2 + \frac{1}{24\pi^2}k^2. \quad (78)$$

The integrations over θ, q_0, and q are straightforward (in this order), but the result we obtain, $I(K) - I(0) = k^2/24\pi^2$, is clearly in contradiction to the result of dimensional regularization. This result turns out to be independent of k_0 and can thus trivially be continued to Minkowski space leading to a nonzero value on the light cone. It turns out that this is a consequence of having introduced a cutoff procedure that violates Euclidean rotation invariance for the expression $I(K)$.

Thus, if one has to split frequency and momentum, one should still do it in a Euclidean-invariant way:

$$\begin{aligned} I(K) &= \frac{2\pi}{(2\pi)^4}\int_0^\Lambda dq \int_{-i\sqrt{\Lambda^2-q^2}}^{i\sqrt{\Lambda^2-q^2}} \frac{dq_0}{i} \\ &\quad \times \int_{-1}^{1} dx \frac{q^2}{(q_0-k_0)^2-(q^2+k^2-2qkx)} \\ &= \frac{\pi}{(2\pi)^4}\frac{1}{k}\int_0^\Lambda dqq \int_{-i\sqrt{\Lambda^2-q^2}}^{i\sqrt{\Lambda^2-q^2}} \frac{dq_0}{i} \\ &\quad \times \log\frac{(q_0-k_0)^2-(q-k)^2}{(q_0-k_0)^2-(q+k)^2}. \end{aligned} \tag{79}$$

The angular integration along $x = \cos\theta$ poses no problem for imaginary $q_0 = i\omega_n$ and $k_0 = i\omega_l$ as the integrand is finite and continuous for all $-1 \le x \le 1$. The integration along q_0 is more problematic as the integrand

$$\log\frac{(q_0-k_0)^2-(q-k)^2}{(q_0-k_0)^2-(q+k)^2} \tag{80}$$

has singularities at $q_0 = k_0 \pm |q \pm k|$ and branch cuts which might interfere with the integration path for an external Minkowski $K^\mu = (\omega, k)$. The particular form of writing (80) this way [i.e. not splitting up the logarithm $\log(X/Y)$ into $\log X - \log Y$] leads to an analytic structure in the q_0 complex plane as shown in Fig. 8: a branch cut connecting the left two singularities and a branch cut connecting the rightmost two singularities. Note that if we start with purely imaginary k_0, the q_0 integration poses no problem since all singularities and branch cuts are away from the imaginary integration axis (except for $q = k$).

In order to evaluate (79) on the light cone, we have to rotate k_0 from the imaginary to the real axis $k_0 = i\omega_l \to \omega + i\epsilon$. By doing so, all four singularities will move to the right, and one of them will eventually cross the integration path when $\mathrm{Re}\, k_0 > |q-k|$. We want $I(K)$ to stay an analytic function. This is only possible if we avoid singularities and branch cuts by deforming the (numerical) integration path as shown in Fig. 9. A deformation of a complex path that does not cross poles, singularities, or branch cuts, will not change the result of a complex integration.

Note that $q = k$ gives a "pinch singularity," that is a point where in Fig. 8 two singularities pinch the integration path. It turns out that in our case this singular point corresponds to a discontinuity of the first derivative of the q integrand, but is otherwise harmless for the q integration. Also note that, when $q > 2k = 2k_0$, we do not have to deform the integration path as the point $B = k_0 - |q-k| < 0$ in Fig. 9 stays on the left side of the integration path even on the light cone. We can choose the integration path such that all path deformation is performed for $Q_E = \sqrt{-q_0^2+q^2} < \Lambda_1$ and no path deformation needed for $Q_E > \Lambda_1$ as long as the intermediate cutoff $\Lambda_1 > 2k$.

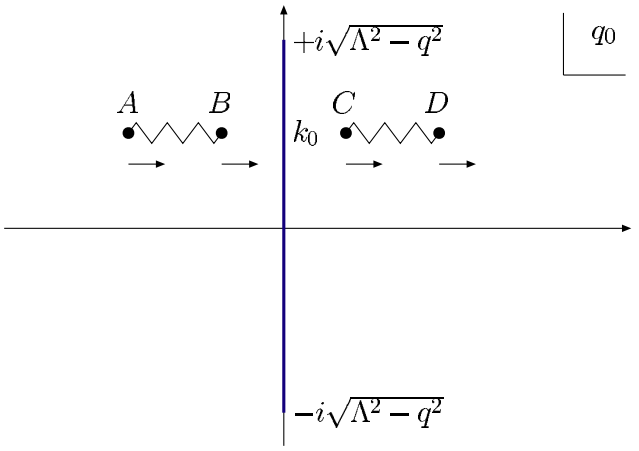

FIG. 8 (color online). The branch cut structure for the q_0 integration in (79) with the logarithmic singularities at $A = k_0 - |q+k|$, $B = k_0 - |q-k|$, $C = k_0 + |q-k|$, $D = k_0 + |q+k|$. For purely imaginary k_0 (in the plot just between B and C), the integration path runs from $-i\sqrt{\Lambda^2-q^2}$ to $i\sqrt{\Lambda^2-q^2}$ and does not cross any logarithmic branch cut.

Performing the numerical integration with the modified path indeed gives the desired result $I(K) - I(0) = 0$ also on the light cone, in accordance with dimensional regularization. Blindly integrating across the branch cut with-

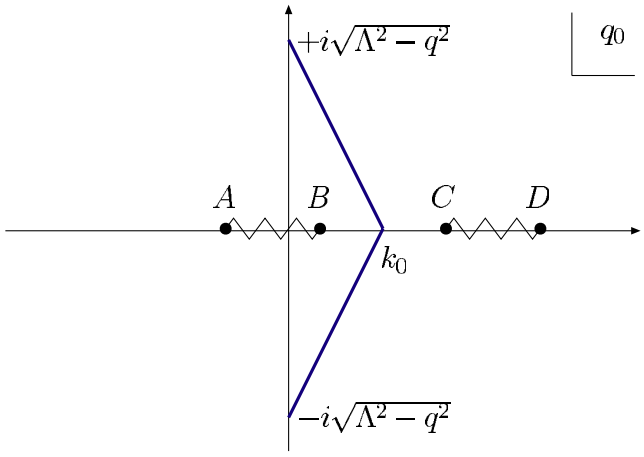

FIG. 9 (color online). As the rotation $k_0 = i\omega \to \omega$ moves all the singularities at the same time, we should also deform the integration path in order to avoid crossing a singularity or branch cut.

out deforming the integration path would give a wrong, nonvanishing result on the light cone.

2. Full cutoff implementation

We can now perform the angular integration in the vacuum contributions (76) and obtain

$$\begin{aligned}\bar{\Sigma}_{\mathrm{L}}^{\mathrm{vac}}(K) &= -4g^2C_f\frac{2\pi}{(2\pi)^4}\int_0^\Lambda dqq^2\int_{-i\sqrt{\Lambda^2-q^2}}^{i\sqrt{\Lambda^2-q^2}}\frac{dq_0}{i}G_{\mathrm{L}}(Q)\\ &\quad\times\left[1-\frac{(q_0-k_0)(q_0-3k_0)-q^2+k^2}{4kq}\log\frac{(q_0-k_0)^2-(q-k)^2}{(q_0-k_0)^2-(q+k)^2}\right],\\ \bar{\Sigma}_{\mathrm{T}}^{\mathrm{vac}}(K) &= -8g^2C_f\frac{2\pi}{(2\pi)^4}\int_0^\Lambda dqq^2\int_{-i\sqrt{\Lambda^2-q^2}}^{i\sqrt{\Lambda^2-q^2}}\frac{dq_0}{i}G_{\mathrm{T}}(Q)\\ &\quad\times\left[-\frac{(q_0-k_0)^2+q^2-k^2}{2q^2}+\frac{((q_0-k_0)^2-k^2)^2-q^2(4k_0(k_0-q_0)+q^2)}{8kq^3}\log\frac{(q_0-k_0)^2-(q-k)^2}{(q_0-k_0)^2-(q+k)^2}\right].\end{aligned}\tag{81}$$

The bare propagator $\Delta_0(P)=\Delta_0(K-Q)$ gives the same logarithmic expression of the form (80) as in our example. But $G_{\mathrm{L}}(Q)$ and $G_{\mathrm{T}}(Q)$, which contain the gluon self-energies Π_{L} and Π_{T}, provide additional branch cut structures along the real q_0 axis such that the path deformation is further restricted as shown in Fig. 10. The integration path goes from q_0: $-i\sqrt{\Lambda^2-q^2}\to 0\to k_0(=\omega+i\epsilon)\to i\sqrt{\Lambda^2-q^2}$.

Another numerical subtlety is involved: Keeping ϵ small but fixed will limit the upper integration bound of the q_0 integration to $i\sqrt{\Lambda^2-q^2}>i\epsilon$ (see Fig. 10) which means that the q-integration is limited to $0\le q<\sqrt{\Lambda^2-\epsilon^2}$. The error introduced by this turns out to be at least of the order $O(\epsilon^2)$.

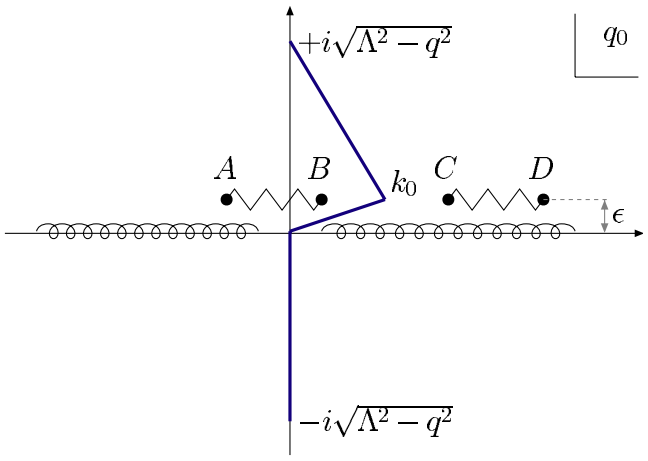

FIG. 10 (color online). A general propagator with self-energy Π will introduce additional cuts and poles along the real q_0 axis. In this case, the integration has to go through the origin and k_0 has to be shifted slightly off the real axis to $k_0=\omega+i\epsilon$.

C. Renormalization

1. Large-N_f limit

As already mentioned, the disappearance of the counterterms δZ_ψ and δM from the entropy formula indicates that $\mathrm{Re}\,\bar{\Sigma}_{\mathrm{vac}}$ has to be finite on the light cone. Since the propagator G used to compute this quantity contains a Landau pole, we have to be more specific about what we call "finite." $\mathrm{Re}\,\bar{\Sigma}_{\mathrm{vac}}$ is computed with an explicit Euclidean-invariant cutoff $\Lambda\ll\Lambda_{\mathrm{L}}$. The finiteness of $\mathrm{Re}\,\bar{\Sigma}_{\mathrm{vac}}$ means that it is insensitive to Λ in a broad region of momenta $T\ll\Lambda\ll\Lambda_{\mathrm{L}}$. In order to understand this more explicitly, we can use the linearity of $\mathrm{Re}\,\bar{\Sigma}_{\mathrm{vac}}$ with respect to G in order to write $\mathrm{Re}\,\bar{\Sigma}_{\mathrm{vac}}=\mathrm{Re}\,\bar{\Sigma}_{\mathrm{vac}}[G_{\mathrm{vac}}]+\mathrm{Re}\,\bar{\Sigma}_{\mathrm{vac}}[G-G_{\mathrm{vac}}]$. Using the asymptotic behavior of Π_{th}, one can check that the second term of this expression is insensitive to Λ. Thus we only need to check the finiteness of $\mathrm{Re}\,\bar{\Sigma}_{\mathrm{vac}}[G_{\mathrm{vac}}]$ on the light cone.

To do so, we start from Eqs. (81) and transform the integration variables to 4-dimensional variables according to

$$\begin{aligned}&\int_0^\Lambda dqq^2\int_{-i\sqrt{\Lambda^2-q^2}}^{i\sqrt{\Lambda^2-q^2}}\frac{dq_0}{i}f(q_0,q)\\ &\quad=\int_0^\Lambda dQ_EQ_E^3\int_0^\pi d\xi\sin^2\xi f(iQ_E\cos\xi,Q_E\sin\xi).\end{aligned}\tag{82}$$

The integrand can then be expanded for large Q_E and, since in the vacuum $G_{\mathrm{T}}(Q_E)=G_\ell(Q_E)=-G_{\mathrm{L}}(Q_E)/\sin^2\xi=(Q_E^2+\Pi_{\mathrm{vac}}(Q_E^2))^{-1}$ is independent of ξ, we can perform the ξ integration and obtain

$$\mathrm{Re}\,\bar{\Sigma}^{\mathrm{vac}}_{\mathrm{L}}(K) = -4g^2C_f\frac{2\pi}{(2\pi)^4}\int_0^\Lambda dQ_E Q_E^3 G_\ell(Q_E)\frac{\pi}{3}\Big[-\frac{4k^2}{Q_E^2}+\frac{8k^4}{5Q_E^4}-\frac{4k^2(9k^4+42k^2k_0^2-35k_0^4)}{35Q_E^6}+O\Big(\frac{1}{Q_E^8}\Big)\Big],$$
$$\mathrm{Re}\,\bar{\Sigma}^{\mathrm{vac}}_{\mathrm{T}}(K) = -8g^2C_f\frac{2\pi}{(2\pi)^4}\int_0^\Lambda dQ_E Q_E^3 G_{\mathrm{T}}(Q_E)\frac{\pi}{6}\Big[\frac{k^2+3k_0^2\pi}{Q_E^2}-\frac{8k^4\pi}{5Q_E^4}+\frac{8(k^6+7k^4k_0^2)\pi}{35Q_E^6}+O\Big(\frac{1}{Q_E^8}\Big)\Big]. \quad (83)$$

The first term of each expansion is logarithmically divergent if transverse and longitudinal parts are taken separately. Only when adding the components together to form $\bar{\Sigma}^{\mathrm{vac}}(K) = \bar{\Sigma}^{\mathrm{vac}}_{\mathrm{L}}(K) + \bar{\Sigma}^{\mathrm{vac}}_{\mathrm{T}}(K)$, the logarithmic divergence vanishes on the light cone $k_0^2 = k^2$:

$$\mathrm{Re}\,\bar{\Sigma}^{\mathrm{vac}}(K) = -4g^2C_f\frac{2\pi^2}{(2\pi)^4}\int_0^\Lambda dQ_E Q_E^3 G_{\mathrm{vac}}(Q_E) \times\Big[\frac{k_0^2-k^2}{Q_E^2}+\frac{4k^2(k_0^2-k^2)(k^2+5k_0^2)}{15Q_E^6} + O\Big(\frac{1}{Q_E^8}\Big)\Big]. \quad (84)$$

2. HTL approximation

Unlike the case of large N_f, the disappearance of the counterterms δZ_ψ and δM from the entropy formula cannot be taken as an indication of the finiteness of $\mathrm{Re}\,\bar{\Sigma}_{\mathrm{vac}}[\hat{G}]$. This is because $\hat{G}$ is built from approximations of Feynman diagrams which may change its asymptotic behavior. However, one can check that both transverse and longitudinal HTL propagators can be expanded in the form

$$\hat{G}(Q_E,\xi) = \frac{1}{Q_E^2}\Big\{1+f(\xi)\frac{m_D^2}{Q_E^2}+O\Big(\frac{m_D^4}{Q_E^4}\Big)\Big\}. \quad (85)$$

The additional angular dependence $f(\xi)$ is suppressed by a factor m_D^2/Q_E^2 at large Q_E and therefore does not influence the leading logarithmic divergent behavior of Eqs. (83) and (84): the leading divergence still vanishes on the light cone.

V. NUMERICAL RESULTS

A. Numerical implementations

The evaluation of Eq. (76) requires three consecutive numerical integrations (of which one is given by the complex path described earlier) in order to obtain one value of $\Sigma(\omega = k; g^2_{\mathrm{eff}})$. With our implementation this takes of the order of 10 hours on a current PC (3 GHz). This has to be integrated over to obtain the fermionic contribution to the entropy $S_{\mathrm{fermion}}(g^2_{\mathrm{eff}})$ for one point of g^2_{eff}. Part of the code was therefore ported to run in parallel and final results could be obtained on the ECT* Teraflop Cluster within a couple of weeks that would have taken years on a standard PC.

It turns out that the numeric cancellation in the integrand (76) for large q and (imaginary) q_0 works best if one integrates over 4-dimensional Euclidean spheres at fixed $Q_E = \sqrt{-q_0^2+q^2}$ first. No path deformation is needed as long as $Q_E > 2k$ as was discussed at the end of Sec. IV B 1. Unfortunately, the path deformation for 4-dimensional angular variables turns out to be much more involved (the corresponding deformed path could become infinitely long due to inverse trigonometric functions), such that a hybrid approach seems a good compromise between simple path-deformation for small Q_E and good convergence properties for larger Q_E:

$$\int_0^\Lambda d^4q = \int_0^{\Lambda_1} d^4q + \int_{\Lambda_1}^\Lambda d^4q = \int_0^{\Lambda_1} dq q^2 \int_{-i\sqrt{\Lambda_1^2-q^2}}^{i\sqrt{\Lambda_1^2-q^2}} \frac{dq_0}{i}\int d\Omega_2 + \int_{\Lambda_1}^\Lambda dQ_E Q_E^3 \int d\Omega_3 \quad (86)$$

where Λ_1 is an intermediate cutoff to be chosen such that $2k < \Lambda_1 \ll \Lambda$ (in our implementation we chose $\Lambda_1 = 2.1k$), and $\int d\Omega_2$ and $\int d\Omega_3$ denote the 3- and 4-dimensional angular integrations. Practically, yet another cutoff $\Lambda_1 < \Lambda_2 < \Lambda$ is introduced, above which the angular integration $\int d\Omega_3$ is performed analytically on the high-temperature series expansion. This series expansion is also used to show that neither large-N_f nor HTL gluon self-energies contain logarithmically divergent pieces for high momentum shells.

In order to correctly integrate all peaks along the complex path, the routine for complex path integration is enhanced by providing information about analytically or numerically known positions in the complex plane of poles of the propagator, $\omega_{\mathrm{L}}(q)$ and $\omega_{\mathrm{T}}(q)$ [48], singularities of the logarithms and other singular points. The integration path is divided into smaller segments in the vicinity of such points where the integrand can rapidly change its value by orders of magnitude.

B. Asymptotic thermal quark masses

Figures 11–13 show the results of a numerical calculation of the asymptotic thermal quark mass squared $M_\infty^2(k) \equiv 2k\,\mathrm{Re}\,\Sigma(k_0 = k)$ for three different values of the coupling $g^2_{\mathrm{eff}}(\bar{\mu}_{\overline{\mathrm{MS}}} = \pi T) = 4$, 9, and 16, and normalized by T^2C_f/N_f. (Recall that this quantity is of order N_f^{-1}, and it contributes to the entropy only because there are N_f fermions.) The exact (nonperturbative) result obtained in the large-N_f limit is given by the full lines.

As anticipated, the asymptotic thermal quark mass squared is a nontrivial function of momentum. It is maximal for $k \sim T$ and decays for large $k \gg T$. The fact that it

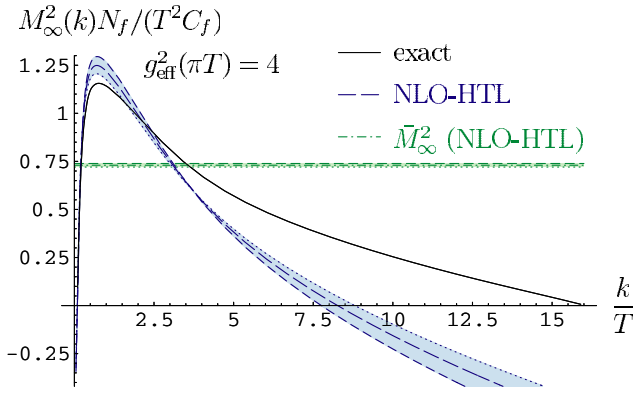

FIG. 11 (color online). Asymptotic thermal quark mass squared (real part of the fermionic self-energy on the light cone) as a function of k/T for $g_{\rm eff}^2(\pi T) = 4$. The exact large-N_f result is compared to the NLO-HTL calculation and its relevant average value. The renormalization scale $\bar{\mu}_{\overline{\rm MS}}$ is varied around the FAC-m scale by factors of 2 (see text).

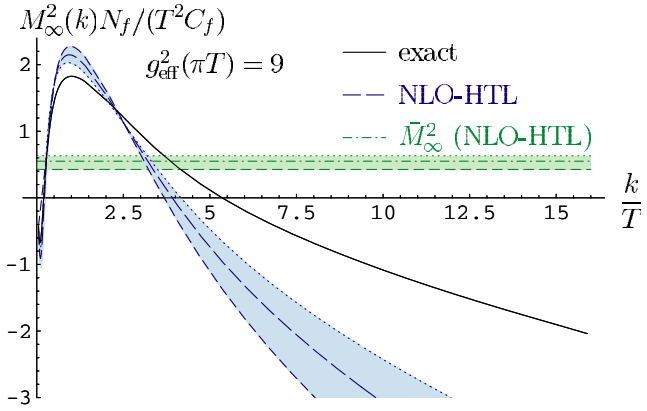

FIG. 12 (color online). Same as Fig. 11 for $g_{\rm eff}^2(\pi T) = 9$.

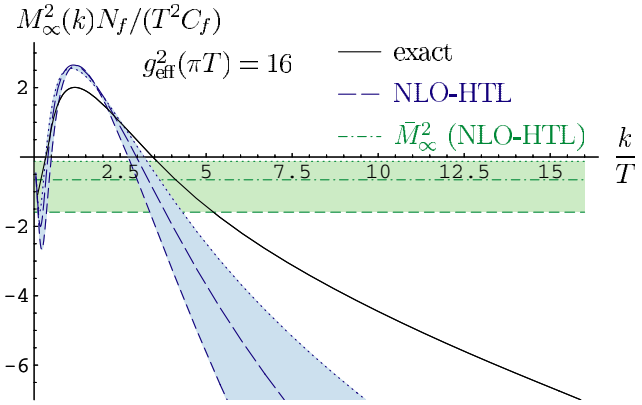

FIG. 13 (color online). Same as Fig. 11 for $g_{\rm eff}^2(\pi T) = 16$.

vanishes and even becomes negative at very small momentum is not to be taken seriously. $M_\infty(k)$ is referred to as asymptotic thermal quark mass, because only at hard $k \gtrsim T$ does this have the interpretation of a quasiparticle mass; for smaller k one would have to search for a self-consistently determined pole of the dressed quark propagator rather than evaluate the quark self-energy on the tree-level mass shell, i.e. the light cone. $M_\infty^2(k)$ however also becomes negative at very large momenta, $k \gg T$. This means that the dispersion law for hard fermionic modes eventually turns spacelike, which does not necessarily signal an inconsistency of the theory. In fact, the group velocity remains smaller than the speed of light for all $k \gtrsim T$. Negative $M_\infty^2(k)$ however opens up the possibility for Čerenkov radiation and thus means that at the corresponding values of k there is a qualitative difference to the leading-order result $\hat{M}_\infty^2 = \frac{1}{2} g_{\rm eff}^2 C_f T^2/N_f$.

The next-to-leading order result as obtained in HTL-resummed perturbation theory (i.e., replacing the full gauge boson propagator in the quark self-energy by its HTL approximation) is given by the dashed lines in Figs. 11–13. Qualitatively, the HTL result is similar to the exact large-N_f result. Quantitatively, like every perturbative result, it has a dependence on the renormalization scale. The HTL result is displayed for a range of renormalization scales $\bar{\mu}_{\overline{\rm MS}}$ centered at $\bar{\mu}_{\rm FAC-m} = \exp(\frac{1}{2} - \gamma_{\rm E})\pi T \approx 0.926\pi T$ which is the scale of fastest apparent convergence with respect to the effective mass parameter $m_{\rm E}$ in dimensional reduction [3]. The upper (dotted) limiting lines of the shaded bands correspond to $\frac{1}{2} \times \bar{\mu}_{\rm FAC-m}$, while the lower (dashed) limiting lines correspond to $2 \times \bar{\mu}_{\rm FAC-m}$. The renormalization scale dependence is seen to increase with the coupling $g_{\rm eff}^2$, and also in the domain where $k \gg T$. For large values of k, the HTL result for the asymptotic mass squared turns more quickly negative than the full result, but in fact at large values of k the modes are severely suppressed by the Bose-Einstein distribution factor. The range $k \sim T$ is more relevant physically (in particular for the calculation of the entropy to be discussed presently), and here the agreement with the exact large-N_f result is much better.

For the computation of the fermionic contribution to the entropy, the asymptotic thermal mass appears in the form of the weighted average given in Eq. (64). This averaged asymptotic thermal mass is given for the HTL approximation by the flat horizontal bands labeled $\bar{M}_\infty^2$ (NLO-HTL). For the entire range of couplings that we can consider without becoming sensitive to the scale of the Landau pole, the averaged asymptotic quark masses are compared in Fig. 14. The full line is again the exact large-N_f result, given as a function of $g_{\rm eff}^2(\pi T)$. The short-dashed lines correspond to the leading-order HTL value $\hat{M}_\infty^2$ with renormalization scale varied as before. The perturbative next-to-leading order result (65) is given by the longer-dashed lines. Finally, the full NLO-HTL-resummed result, not truncated at order $g_{\rm eff}^3$, is given by the dash-dotted lines.

As one can see in Fig. 14, the NLO-HTL-resummed result represents a considerable improvement over the

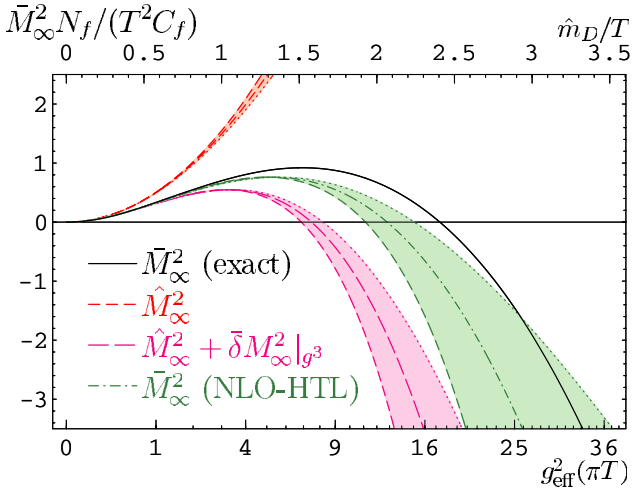

FIG. 14 (color online). Comparison of the averaged asymptotic thermal quark mass squared, $\bar{M}_\infty^2$, in various approximations as explained in the text. The renormalization scale $\bar{\mu}_{\overline{\rm MS}}$ is varied around the FAC-m scale by factors of 2.

HTL-resummed result truncated at order $g_{\rm eff}^3$ for $g_{\rm eff}^2 \gtrsim 4$, which corresponds to $\hat{m}_D/T \gtrsim 1$.

C. Numerical results for the entropy and discussion

Figure 15 shows the numerical results of the entropy calculation. The full line is the entropy density $S = (\partial P/\partial T)_\mu$ as it has been obtained earlier [33–35] by a numerical derivative of the pressure P from Eq. (43) for massless fermions $m = 0$. It is a very nontrivial numerical

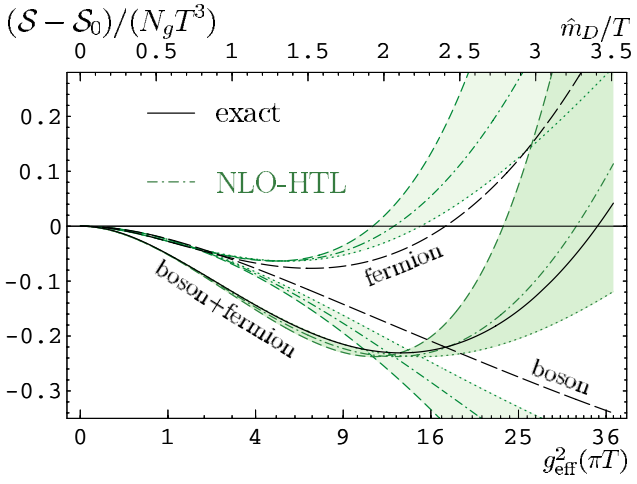

FIG. 15 (color online). Entropy in the large-N_f limit separated into a bosonic and a fermionic part, corresponding, respectively, to the first and second line of Eq. (57). The NLO-HTL approximation to the two parts of the entropy is depicted in dashed lines, where the renormalization scale $\bar{\mu}_{\overline{\rm MS}}$ is varied around the FAC-m scale by factors of 2. The combined NLO-HTL result shows remarkable agreement with the exact large-N_f result for all couplings with HTL Debye mass $\hat{m}_D \lesssim 2.5T$.

test that the result for the entropy as obtained from the Φ-derivable two-loop approximation, Eq. (14), reproduces exactly the same result in the large-N_f limit, as has been discussed in Sec. III A. Indeed, only after implementing the correct path deformation for the calculation of Σ, we have been able to reproduce the entropy to three or four digits, where the accuracy was limited only by the high calculation cost for the multidimensional integrals. In Fig. 15 the two curves lie perfectly on top of each other for the whole range of couplings displayed.

We show the results in a range of couplings $g_{\rm eff}^2(\pi T) \lesssim 36$ where the influence of the Landau pole can be neglected. As in [33–35] we obtain differences in the entropy on the percent level for the largest couplings $g_{\rm eff}^2(\bar{\mu}_{\overline{\rm MS}} = \pi T) \approx 36$ by varying the numerical cutoff $\Lambda^2 = a\Lambda_{\rm L}^2$ in the range $a = 1/4..1/2$.

According to Eq. (57), the large-N_f entropy as well as the HTL approximation thereof is composed of a bosonic and a fermionic contribution. The fermionic one is entirely given by the weighted average (64) of the asymptotic thermal quark mass that we have discussed above and it is reproduced in Fig. 15 by the line marked "fermion," together with its NLO-HTL approximation. The calculation of the bosonic contribution is less demanding computationally. The result is shown by the line marked "boson" in Fig. 15. The HTL approximation to the bosonic contribution does not require NLO corrections to the asymptotic bosonic masses in the large-N_f limit, and it has been calculated completely already in Refs. [21,23]. Evaluated for the range of renormalization scales considered here, it gives the band below the line marked boson. Perhaps fortuitously, the errors of the bosonic contribution to the HTL approximation of the entropy are opposite in sign from those of the fermionic contribution. The sum total turns out to reproduce the exact result with astounding accuracy up to $g_{\rm eff}^2 \sim 16$. For larger coupling the renormalization scale dependence quickly becomes enormous, however the central value determined by the optimized scale $\bar{\mu}_{\overline{\rm MS}} = \bar{\mu}_{\rm FAC-m}$ remains amazingly close to the exact result for all values of $g_{\rm eff}$. In Ref. [35] a similarly successful approximation was constructed by using optimized renormalization scales on a perturbative result, which however required to include all contributions up to and including order $g_{\rm eff}^6$.

In Fig. 16 the exact and the NLO-HTL result is also compared to simpler approximations. The short-dashed lines give the strictly perturbative result up to and including order $g_{\rm eff}^3$, the longer-dashed lines labeled "NLA" (next-to-leading approximation) show the result of comparing the bosonic HTL entropy with a perturbative approximation to the averaged asymptotic thermal quark mass presented before in Ref. [36]. The latter corresponds to the large-N_f limit of the HTL-resummed entropies obtained in Refs. [21–23]. While this does lead to an important improvement for couplings such that $\hat{m}_D/T \lesssim 1.5$, it is re-

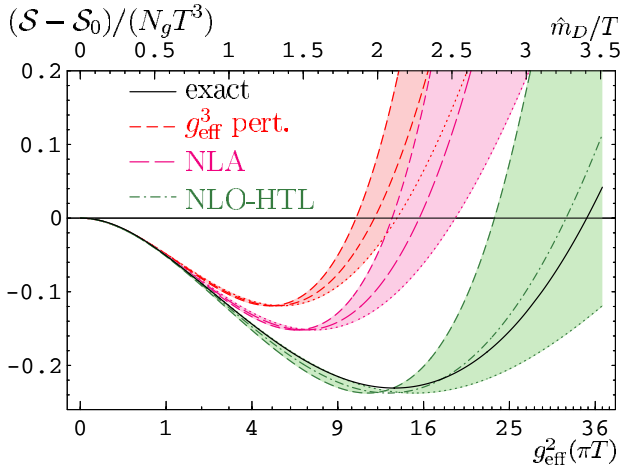

FIG. 16 (color online). Entropy in the large-N_f limit, comparing the exact large-N_f result to the strictly perturbative expansion through order $g^3_{\rm eff}$, the NLA result, and the NLO-HTL result. The renormalization scale $\bar{\mu}_{\overline{\rm MS}}$ is varied around the FAC-m scale by factors of 2.

markable that a complete HTL resummation in the asymptotic thermal mass can push the range where HTL resummation works well up to $\hat{m}_D/T \sim 2.5$.

VI. CONCLUSIONS AND OUTLOOK

We have calculated the large-N_f limit of the entropy of ultrarelativistic gauge theories by evaluating separately the contributions from bosonic and fermionic quasiparticles. Since in the large-N_f limit, the 2-loop Φ-derivable approximation becomes exact, this allowed us to assess the error that is being made when fully dressed propagators and self-energies are replaced by their HTL approximations.

In the case of the bosonic contributions, these approximations correspond to replacing a full fermion loop in the dressed gluon propagator by its HTL approximation. The fermionic contributions to the entropy, on the other hand, involve the momentum-dependent asymptotic thermal quark mass where the HTL approximation has to be carried to next-to-leading order. In both cases the HTL approximation turned out to give remarkably good results when compared with the exact large-N_f results, even for fairly large coupling. Combining these contributions, the final result for the entropy in the NLO-HTL approximation turned out to be amazingly accurate up to $\hat{m}_D/T \sim 2.5$, and even beyond when the renormalization scale is fixed by the requirement of fastest apparent convergence of the electric mass in dimensional reduction. Its quality is then comparable to optimized perturbative results including terms through order $g^6_{\rm eff}$. This supports the conclusions of Ref. [49,50] where optimized dimensional-reduction results for QCD to order $g^6\log(g)$ were found to agree well with available lattice data and in turn with the estimates from the HTL entropy.

The improvement achieved by including the full momentum dependence of asymptotic thermal masses and keeping all effects of the resummation of hard thermal loops is encouraging for further developments of this approach. A straightforward extension of the present calculations would be the inclusion of finite quark chemical potential. The calculation of quark densities and quark number susceptibilities [51–53] for small-N_f QCD within NLO-HTL resummation in fact requires exclusively the asymptotic quark thermal masses that were calculated in the present work for zero chemical potential. By also calculating the full momentum-dependent asymptotic gluon masses, one could finally complete the existing HTL results [21–23] for the entropy of full QCD in the 2-loop Φ-derivable approximation.

ACKNOWLEDGMENTS

We would like to thank Edmond Iancu for many fruitful discussions and collaboration in the earlier stages of the present work. Urko Reinosa has been supported by the Austrian Science Fund FWF, Project No. P16387-N08.

APPENDIX A: MATSUBARA SUMS

1. Gluon self-energy

The gluon self-energy to leading order in N_f is given by

$$\Pi^{\mu\nu}_{\rm b}(Q) = g^2_{\rm eff}\,{\rm tr}\sum\!\!\!\!\!\!\int_K \gamma^\mu S_0(K)\gamma^\nu S_0(P), \qquad \text{(A1)}$$

with $P = K - Q$. It is convenient to split this self-energy into a vacuum and a thermal piece $\Pi_{\rm b} = \Pi_{\rm b,vac} + \Pi_{\rm th}$ (the label "b" stands for bare and is here to remind that the vacuum piece contains UV divergences). The vacuum piece is simply obtained by replacing the discrete Matsubara sum by a continuous integral, thus leading to a 4-dimensional Euclidean integral:

$$\Pi^{\mu\nu}_{\rm b,vac}(Q) = g^2_{\rm eff}\,{\rm tr}\int_{K_{\rm E}} \gamma^\mu S_0(K)\gamma^\nu S_0(P). \qquad \text{(A2)}$$

The thermal piece is obtained after performing the Matsubara sums and separating the thermal dependent pieces. A convenient way to proceed is to introduce the spectral representation (7) for each of the fermionic propagators:

$$\Pi^{\mu\nu}_{\rm b}(Q) = g^2_{\rm eff}\,{\rm tr}\int_{p_0}\int_{k_0}\int_{\mathbf{k}} \gamma^\mu(\not{K} + M)\rho_0(K)\gamma^\nu(\not{P} + M) \times \rho_0(P)\frac{1}{\beta}\sum_l \frac{1}{(k_0 - i\omega_l)(p_0 - i\omega_m)}, \qquad \text{(A3)}$$

where $\omega_m = \omega_l - \omega_n$ and $q_0 = i\omega_n$. One can now easily perform the Matsubara sum and extract the thermal dependent part:

$$\frac{1}{\beta}\sum_l \frac{1}{(k_0 - i\omega_l)(p_0 - i\omega_l + i\omega_n)} = \frac{-f(k_0) + f(p_0)}{p_0 - k_0 + i\omega_n}$$
$$= \frac{-\epsilon(k_0)f(|k_0|) + \epsilon(p_0)f(|p_0|)}{p_0 - k_0 + i\omega_n} + \text{vac}, \quad \text{(A4)}$$

where we have used $f(k_0) = \theta(-k_0) + \epsilon(k_0)f(|k_0|)$. The thermal part of the gluon self-energy now reads (we do not use the label "b" since this contribution is UV finite)

$$\Pi^{\mu\nu}_{\text{th}}(Q) = g^2_{\text{eff}}\,\text{tr}\int_{p_0}\int_{k_0}\int_{\mathbf{k}} \gamma^\mu(\not{K} + M)\rho_0(K)\gamma^\nu(\not{P} + M) \times \rho_0(P)\frac{-\epsilon(k_0)f(|k_0|) + \epsilon(p_0)f(|p_0|)}{p_0 - k_0 + q_0}. \quad \text{(A5)}$$

Using the spectral representation for the fermion propagator, the parity properties of $\Pi^{\mu\nu}$ together with a straightforward change of variables (which is justified since the cutoff can be sent to infinity in the thermal contribution), one obtains

$$\Pi^{\mu\nu}_{\text{th}}(Q) = -2g^2_{\text{eff}}\,\text{tr}\int_K \gamma^\mu(\not{K} + M)\sigma_0(K)\gamma^\nu S_0(K - Q), \quad \text{(A6)}$$

with $\sigma_0(K) = \epsilon(k_0)f(|k_0|)\rho_0(K)$.

2. Fermion self-energy

In this section, we compute the fermionic Matsubara sums:

$$\bar{\Sigma}_{\text{L}}(K) = -4g^2C_f\sum\!\!\!\!\!\!\int_Q [k_0p_0 + \mathbf{k}\cdot\mathbf{p}]\Delta_0(P)G_{\text{L}}(Q),$$
$$\bar{\Sigma}_{\text{T}}(K) = -8g^2C_f\sum\!\!\!\!\!\!\int_Q [k_0p_0 - (\hat{\mathbf{q}}\cdot\mathbf{k})(\mathbf{p}\cdot\hat{\mathbf{q}})]\Delta_0(P)G_{\text{T}}(Q), \quad \text{(A7)}$$

with $P = K - Q$. To that aim, we use the spectral representations (7) and (18). The longitudinal part gives

$$\bar{\Sigma}_{\text{L}}(K) = 4g^2C_f\int_{\mathbf{q}}\int_{p_0}[k_0p_0 + \mathbf{k}\cdot\mathbf{p}]\frac{1}{\mathbf{q}^2}\rho_0(P)\frac{1}{\beta}\sum_n\frac{1}{p_0 - i\omega_m} - 4g^2C_f\int_{\mathbf{q}}\int_{p_0}\int_{q_0}[k_0p_0 + \mathbf{k}\cdot\mathbf{p}] \times \rho_0(P)\rho_{\text{L}}(Q)\frac{1}{\beta}\sum_n\frac{1}{(p_0 - i\omega_m)(q_0 - i\omega_n)}, \quad \text{(A8)}$$

where $i\omega_m = i\omega_l - i\omega_n$ and $k_0 = i\omega_l$. The Matsubara sums give

$$\frac{1}{\beta}\sum_n\frac{1}{p_0 - i\omega_l + i\omega_n} = -n(-p_0 + i\omega_l) = f(-p_0) = -\epsilon(p_0)f(|p_0|) + \text{vac},$$
$$\frac{1}{\beta}\sum_n\frac{1}{(p_0 - i\omega_l + i\omega_n)(q_0 - i\omega_n)} = \frac{n(q_0) + f(-p_0)}{p_0 + q_0 - i\omega_l} = \frac{\epsilon(q_0)n(|q_0|) - \epsilon(p_0)f(|p_0|)}{p_0 + q_0 - i\omega_l} + \text{vac}, \quad \text{(A9)}$$

where we have used $f(-p_0) = \theta(p_0) - \epsilon(p_0)f(|p_0|)$ and $n(q_0) = -\theta(-q_0) + \epsilon(q_0)n(|q_0|)$. Then, we have

$$\bar{\Sigma}_{\text{L,th}}(K) = -4g^2C_f\int_{\mathbf{q}}\int_{p_0}[k_0p_0 + \mathbf{k}\cdot\mathbf{p}] \times\frac{1}{\mathbf{q}^2}\rho_0(P)\epsilon(p_0)f(|p_0|) - 4g^2C_f\int_{\mathbf{q}}\int_{p_0}\int_{q_0}[k_0p_0 + \mathbf{k}\cdot\mathbf{p}]\rho_0(P)\rho_{\text{L}}(Q) \times\frac{\epsilon(q_0)n(|q_0|) - \epsilon(p_0)f(|p_0|)}{p_0 + q_0 - k_0}, \quad \text{(A10)}$$

We can now use the spectral representations backwards to write [we change variables in the second line $\mathbf{q} \to \mathbf{p}$, this is possible since the cutoff can be sent to infinity in the thermal contributions; the first line then cancels against the $1/\mathbf{q}^2$ contribution from Eq. (18)]:

$$\bar{\Sigma}_{\text{L,th}}(K) = 4g^2C_f\int_P[k_0p_0 + \mathbf{k}\cdot\mathbf{p}]\sigma_0(P)G_{\text{L}}(K - P) - 4g^2C_f\int_Q[k_0(k_0 - q_0) + \mathbf{k}\cdot\mathbf{p}] \times\Delta_0(K - Q)\sigma_{\text{L}}(Q), \quad \text{(A11)}$$

with $\sigma_0(P) = \epsilon(p_0)f(|p_0|)\rho_0(P)$ and $\sigma_{\text{L}}(Q) = \epsilon(q_0)n(|q_0|)\rho_{\text{L}}(Q)$. In the same way, one obtains for the transverse piece

$$\bar{\Sigma}_{\text{T,th}}(K) = 8g^2C_f\int_P[k_0p_0 - (\hat{\mathbf{q}}\cdot\mathbf{k})(\mathbf{p}\cdot\hat{\mathbf{q}})]\sigma_0(P)G_{\text{T}}(K - P) - 8g^2C_f\int_Q[k_0(k_0 - q_0) - (\hat{\mathbf{q}}\cdot\mathbf{k})(\mathbf{p}\cdot\hat{\mathbf{q}})] \times\Delta_0(K - Q)\sigma_{\text{T}}(Q), \quad \text{(A12)}$$

with $\sigma_{\text{T}}(Q) = \epsilon(q_0)n(|q_0|)\rho_{\text{T}}(Q)$.

APPENDIX B: RELATION BETWEEN Σ_+ AND Σ_-

Σ_+ and Σ_- from Eq. (24) can be related to each other by application of the Schwarz reflection principle: It can be shown that $b(k_0 = i\omega_l, k) = b^*(i\omega_l, k)$ is a purely real quantity in Euclidean space (i.e. along the imaginary axis $k_0 = i\omega_l$), as is $ia(i\omega_l, k) = -ia^*(i\omega_l, k)$. The Schwarz reflection principle implies that in a rotation from Euclidean to Minkowski space $k_0 = i\omega_l \to \omega + i\epsilon$ on the one hand and $k_0 = i\omega_l \to -\omega + i\epsilon$ on the other, the

values of b can be related via $b(k_0 = \omega + i\epsilon, k) = b^*(-\omega + i\epsilon, k)$. The same holds for $ia(\omega + i\epsilon, k) = -ia^*(-\omega + i\epsilon, k)$. Combining the two results as in $\Sigma_\pm = b \pm a$ (and $\Sigma^*_\pm = b^* \pm a^*$) gives

$$\Sigma_+(\omega + i\epsilon, k) = \Sigma^*_-(-\omega + i\epsilon, k). \tag{B1}$$

This result is of course also valid for finite ϵ, i.e. all $\omega \geq 0$ and $\epsilon > 0$. Particularly for $\epsilon \to 0$ this implies

$$\begin{aligned}\mathrm{Re}\,\Sigma_+(\omega = k, k) &= \mathrm{Re}\,\Sigma_-(\omega = -k, k) \\ &= \frac{1}{4k}\,\mathrm{Re}\,\bar{\Sigma}(\omega = \pm k, k).\end{aligned} \tag{B2}$$

[1] P. Arnold and C.-X. Zhai, Phys. Rev. D **51**, 1906 (1995).
[2] C.-X. Zhai and B. Kastening, Phys. Rev. D **52**, 7232 (1995).
[3] E. Braaten and A. Nieto, Phys. Rev. D **53**, 3421 (1996).
[4] K. Kajantie, M. Laine, K. Rummukainen, and Y. Schröder, Phys. Rev. D **67**, 105008 (2003).
[5] R. Parwani and H. Singh, Phys. Rev. D **51**, 4518 (1995).
[6] I. T. Drummond, R. R. Horgan, P. V. Landshoff, and A. Rebhan, Nucl. Phys. **B524**, 579 (1998).
[7] B. Kastening, Phys. Rev. D **56**, 8107 (1997).
[8] T. Hatsuda, Phys. Rev. D **56**, 8111 (1997).
[9] G. Cvetič and R. Kögerler, Phys. Rev. D **70**, 114016 (2004).
[10] V. I. Yukalov and E. P. Yukalova, in *Relativistic Nuclear Physics and Quantum Chromodynamics*, edited by A. M. Baldin and V. V. Burov (Joint Institute for Nuclear Research, Dubna, 2000), pp. 238–245.
[11] R. R. Parwani, Phys. Rev. D **63**, 054014 (2001).
[12] R. R. Parwani, Phys. Rev. D **64**, 025002 (2001).
[13] F. Karsch, A. Patkós, and P. Petreczky, Phys. Lett. B **401**, 69 (1997).
[14] J. O. Andersen, E. Braaten, and M. Strickland, Phys. Rev. D **63**, 105008 (2001).
[15] E. Braaten and R. D. Pisarski, Phys. Rev. D **45**, R1827 (1992).
[16] J. Frenkel and J. C. Taylor, Nucl. Phys. **B374**, 156 (1992).
[17] J. O. Andersen, E. Braaten, and M. Strickland, Phys. Rev. Lett. **83**, 2139 (1999).
[18] J. O. Andersen, E. Braaten, E. Petitgirard, and M. Strickland, Phys. Rev. D **66**, 085016 (2002).
[19] J. O. Andersen, E. Petitgirard, and M. Strickland, Phys. Rev. D **70**, 045001 (2004).
[20] J. O. Andersen and M. Strickland, Ann. Phys. (N.Y.) **317**, 281 (2005).
[21] J. P. Blaizot, E. Iancu, and A. Rebhan, Phys. Rev. Lett. **83**, 2906 (1999).
[22] J. P. Blaizot, E. Iancu, and A. Rebhan, Phys. Lett. B **470**, 181 (1999).
[23] J. P. Blaizot, E. Iancu, and A. Rebhan, Phys. Rev. D **63**, 065003 (2001).
[24] J. P. Blaizot, E. Iancu, and A. Rebhan, in *Quark-Gluon Plasma 3*, edited by R. C. Hwa and X.-N. Wang (World Scientific, Singapore, 2003).
[25] A. Peshier, Phys. Rev. D **63**, 105004 (2001).
[26] B. Vanderheyden and G. Baym, J. Stat. Phys. **93**, 843 (1998).
[27] H. van Hees and J. Knoll, Phys. Rev. D **65**, 025010 (2002).
[28] H. van Hees and J. Knoll, Phys. Rev. D **65**, 105005 (2002).
[29] J.-P. Blaizot, E. Iancu, and U. Reinosa, Phys. Lett. B **568**, 160 (2003).
[30] J.-P. Blaizot, E. Iancu, and U. Reinosa, Nucl. Phys. **A736**, 149 (2004).
[31] J. Berges, S. Borsányi, U. Reinosa, and J. Serreau, Phys. Rev. D **71**, 105004 (2005).
[32] J. Berges, S. Borsányi, U. Reinosa, and J. Serreau, hep-ph/0503240.
[33] G. D. Moore, J. High Energy Phys. 10 (2002) 055.
[34] A. Ipp, G. D. Moore, and A. Rebhan, J. High Energy Phys. 01 (2003) 037.
[35] A. Ipp and A. Rebhan, J. High Energy Phys. 06 (2003) 032.
[36] A. Rebhan, in *Strong and Electroweak Matter 2002*, edited by M. G. Schmidt (World Scientific, Singapore, 2003), pp. 157–166.
[37] G. Baym, Phys. Rev. **127**, 1391 (1962).
[38] J. M. Luttinger and J. C. Ward, Phys. Rev. **118**, 1417 (1960).
[39] J. M. Cornwall, R. Jackiw, and E. Tomboulis, Phys. Rev. D **10**, 2428 (1974).
[40] K. A. James and P. V. Landshoff, Phys. Lett. B **251**, 167 (1990).
[41] A. Arrizabalaga and J. Smit, Phys. Rev. D **66**, 065014 (2002).
[42] U. Kraemmer, M. Kreuzer, and A. Rebhan, Ann. Phys. (N.Y.) **201**, 223 (1990).
[43] F. Flechsig and A. K. Rebhan, Nucl. Phys. **B464**, 279 (1996).
[44] H. Schulz, Nucl. Phys. **B413**, 353 (1994).
[45] A. K. Rebhan, Phys. Rev. D **48**, R3967 (1993).
[46] G. Aarts and J. M. Martinez Resco, J. High Energy Phys. 03 (2005) 074.
[47] J.-P. Blaizot and U. Reinosa, hep-ph/0406109.
[48] J.-P. Blaizot, A. Ipp, and A. Rebhan, hep-ph/0508317.
[49] J. P. Blaizot, E. Iancu, and A. Rebhan, Phys. Rev. D **68**, 025011 (2003).
[50] A. Ipp, A. Rebhan, and A. Vuorinen, Phys. Rev. D **69**, 077901 (2004).
[51] J. P. Blaizot, E. Iancu, and A. Rebhan, Phys. Lett. B **523**, 143 (2001).
[52] J. P. Blaizot, E. Iancu, and A. Rebhan, Eur. Phys. J. C **27**, 433 (2003).
[53] A. Rebhan and P. Romatschke, Phys. Rev. D **68**, 025022 (2003).